MULTI-HAZARD INTERACTION ASSESSMENT, CASE STUDY: TROPICAL CYCLONE MARIA
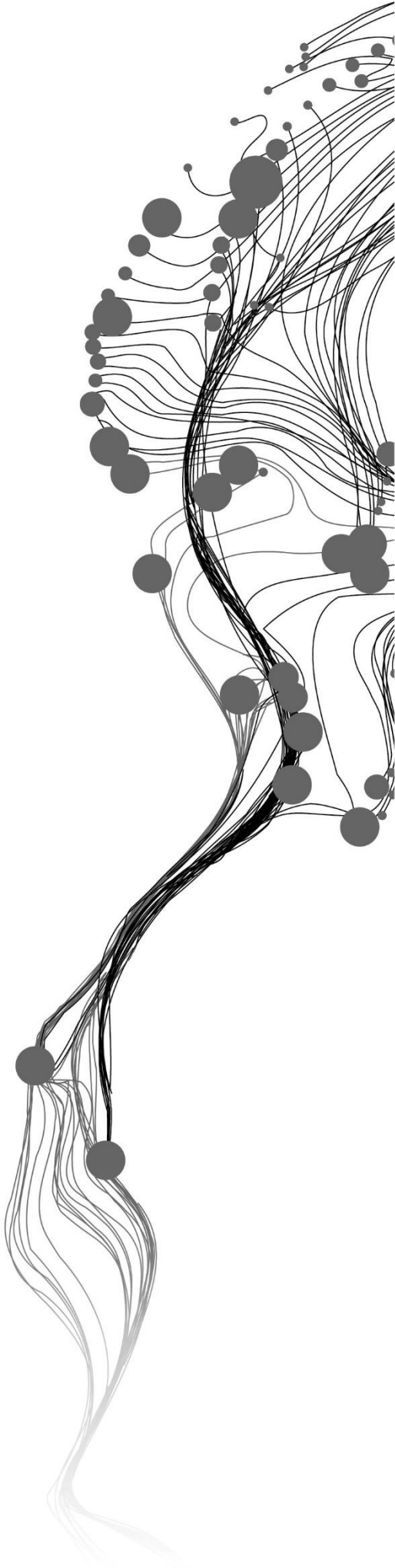
[SWAGATALAXMI DAS]
[July, 2024]

SUPERVISORS:
[Dr. B. van den Bout]
[Dr. ir. J. Ettema]

MULTI-HAZARD INTERACTION ASSESSMENT, CASE STUDY: TROPICAL CYCLONE MARIA

[SWAGATALAXMI DAS]
Enschede, The Netherlands, [July, 2024]

Thesis submitted to the Faculty of Geo-Information Science and Earth Observation of the University of Twente in partial fulfilment of the requirements for the degree of Master of Science in Geo-information Science and Earth Observation.
Specialization: Applied Earth Sciences

SUPERVISORS:
[Dr. B. van den Bout]
[Dr. ir. J. Ettema]

THESIS ASSESSMENT BOARD:
[Prof. dr. C.J. van Westen (Chair)]
[Dr. Lyn Baron (External Examiner, Ministry of Housing and Urban Development, Dominica)]

ABSTRACT

The intensification and frequency of natural hazards pose significant challenges to human societies, requiring an improved understanding of hazards and risks for enhanced disaster risk assessment. Hazards often interact in complex ways, particularly during multi-hazard events like tropical cyclones (TCs). This study focuses on understanding multi-hazard interactions during TC Maria (2017) in Dominica, Caribbean Islands, which involved high winds, storm surges, and landslides, leading to significant socio-economic impacts. TC Maria exemplifies the cascading nature of multi-hazards, where one hazard can trigger subsequent in a chain reaction of events, exacerbating damage. The study aims to analyse these interactions and their effects on structures, emphasizing the importance of recognizing multi-hazard dynamics for accurate risk assessment. Study's findings highlight the intricate interactions between wind, storm surge, and landslide processes during TC Maria, revealing the significant role of wind in triggering subsequent hazards. High winds caused structural damage directly and indirectly, through mechanisms like flying debris and tree falls, which further influenced flood and landslide occurrences. The affected regions exhibited compounded damage due to these interactions, emphasizing the need for multi-hazard-focused risk assessments. By attempting to analyze multi-hazard interactions, this study contributes to a more nuanced understanding of disaster risks, facilitating better resource allocation and emergency planning. The integration of CFD wind modelling approaches, such as CityFFD, offers valuable insights into localized hazard impacts, supporting efforts to build resilient communities against future multi-hazard events.

ACKNOWLEDGEMENTS

TABLE OF CONTENTS

LIST OF FIGURES

LIST OF TABLES

1.   INTRODUCTION

1.1.   Background

The increase in intensity and frequency of hazards in the recent years have become an alarming problem to the human society (Wang et al., 2020). Concepts of hazards and risks should thus be better understood to enhance disaster risk assessment quality, not just to understand present situation but also predict in future the possible scenarios (Ward et al., 2020). Hazards are generally referred to "A process, phenomenon or human activity that may cause loss of life, injury or other health impacts, property damage, social and economic disruption or environmental degradation" (UNISDR, 2009). The event that potentially cause an impact to the society and has a probability to occur within a specific time frame in a specific area with an intensity, is a hazard (Westen & Greiving, 2017). Each hazard or hazard scenarios are hazard events having a certain magnitude or intensity or frequency. Because the hazard are combined with physical, social and environmental factors, societies are vulnerable to loss and damage. When the elements at risk (EAR): people, nature, infrastructure etc. are vulnerable to a potential hazard, there is risk involved in that situation (Gravley, 2001). Thus, they are at risk to the harmful consequences of a hazard depending on the coping mechanisms of the society and characteristics of a given hazard (Ward et al., 2020). The extent or intensity of loss and damage of society from a hazard depends on their coping capacity (UNISDR, 2009). Coping capacity in turn depends on the resources and attributes within or available to the society. When these hazards interact with the vulnerability of elements at risk causing loss of life and destruction to property, then it is termed as a disaster risk (UNISDR, 2009).
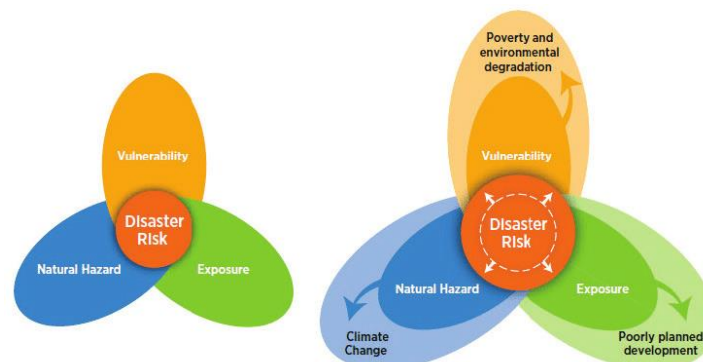
Figure 1: Disaster risk assessment

With high levels of inequality and rapid urbanisation, there is fast environmental degradation which has increased disaster risks (see Figure 1) significantly. By 2030, according to UNDRR, 2022, quantity of disasters will increase to 560 per year compared to current 400 per year scenario. To achieve a reduction of disaster risks, it is pertinent to understand the drivers that cause risk, from a building level to a global scale (Ward et al., 2020). One such way is to understand the characteristics of hazards for present and future scenarios. From the mid-2000s, assessing natural hazards and their characteristics is being undertaken, which is a step forward in reducing risks. Several analysis (UNDRR, 2009, 2011, 2013, 2019, 2022) have been performed by United Nations Office for Disaster Risk Reduction (UNDRR) to globally assess the number of natural hazards in Global Assessment Reports (GAR). The analysis of natural hazard characteristics and its interaction with the society can allow for targeted effort towards mitigation and

preparedness. It can help between understanding estimation of loss making better emergency plans and efficient utilization of resources during future hazards events (Martin, 2021).

However, assessing hazard characteristics is not always easy and straightforward. Many regions of the world are prone to 'multi-hazard' where more than one hazard occur simultaneously with or without time span between each other (Kappes et al., 2012). The term 'multi-hazard' refers to different hazards that affect a place simultaneously, cascadingly or cumulatively over time considering the interrelated effects that takes place (Hochrainer-Stigler et al., 2023). They differ from single-hazard events in the sense that single hazards events are isolated and independent of another hazard event having no interrelationship between them. In simple terms it refers to 'more than one hazard' (Westen & Greiving, 2017). However, multi-hazards are not just overlay of multiple single hazards on each other (Gill & Malamud, 2016). Several hazards coincide in space and time causing an integrated framework and cascading effects between the hazard events. The concept extends to accounting for their potential interactions and relationship between each other (Barrantes, 2018). According to Westen & Greiving, (2017) and Tilloy et al., (2019), there are four prominent different types of hazard interrelations, 1. independent events were two hazards are independent of each other caused due to different trigger factors for instance, earthquake and flood; 2. two different hazards triggered by similar event like, earthquake causing tsunamis in the ocean and landslides on the land; 3. initial hazard changing the disposition of the following hazard for example, earthquake causing landslide which increases chances for mass movement and 4. the cascading hazards. The most difficult kind of multi-hazards to analyse for risk assessment. Cascading hazards comprise of a chain of hazard events interlinked with each other one triggering next event.

Risk analysis of multi-hazard is more complex than single-hazard event since hazard occur simultaneously of consecutively. However, ignoring the interaction between the hazards might cause an incorrect risk analysis and underestimation of disaster risk assessment (Tilloy et al., 2019). A comprehensive risk assessment is crucial for efficient mitigation and preparedness planning and thus, cascading and compounding effects of multi-hazards needs to be taken into consideration. For societies to build back stronger, risk strategies needs to evaluate the interactions between the hazards for a holistic safeguard of communities (Sarker & Adnan, 2024). However, considering different origins (hydrometeorological, geophysical etc.) (Drakes & Tate, 2022) of the interrelated hazards enhances the complexity of analysis. The inaccurate or unavailability of data on the specifics of the multiple hazards occurring simultaneously hinders accurate risk assessment. One of the biggest challenges is quantifying the spatial and temporal relations between the hazards since they are almost difficult to segregate (Sarker & Adnan, 2024). Absence of standardized approaches to multi-hazard risk assessment can also be a prominent challenge in this field. One such extremely difficult and complex to analyse multi-hazard is Tropical cyclone (TC).

As described by Sarker & Adnan, (2024), TCs are a combination of relatively four different hazards: strong winds, storms surge, flood caused by heavy precipitation and landslides (Do & Kuleshov, 2023) having a multi-hazard effect. TCs are extreme weather events, are a major disturbance in various parts of the world (Gardiner et al., 2022). These catastrophic weather phenomena can cause damage to both natural and artificial structures all over the world (Hu & Smith, 2018). According to Gao et al., (2014), damage incurred from TCs have increased in the past few decades. For the past four decades, category 3-5 TCs has increased in proportion globally (IPCC, 2023). TCs do not only disrupt the social and economic livelihood coastal population (Manikanta et al., 2023), but also have a significant negative impact on the recovery of ecosystem and societies from damage (Gardiner et al., 2022). TC damage is incurred by various storm-related phenomena like high-speed winds and long durational high and intense rainfall.

High intensity/length of precipitation can in turn lead to landslides or debris flows called as hydro-morphological hazards (Bryce et al., 2022). In the light of global warming, there is high confidence in the increase of precipitation intensity for TCs (IPCC, 2023). Also, IPCC, (2023) stated that storm surges and thus, flooding can also increase with sea level rise. Importance of studying TCs are thus increasing immensely.

As mentioned, TCs are accompanied of intense precipitation, high wind speed and extreme storm surges. For TC, these events do not occur separately (Hu et al., 2023), and should not be regarded as single hazard events. TCs include more than one hazard event namely, high wind speed, landslides, storm surge, heavy precipitation etc., having complex interaction between each other and capable of substantial increase in loss and damage, which is why TCs are known as multi-hazard events (World Meteorological Organization, 2022). TCs are mostly cascading multi-hazard events as one hazard can become a trigger for another (rainfall causing landslides, landslide leading to dam-break etc.), which are extremely difficult to quantify due to occurrence of simultaneous hazard events.

Interaction between the hazards occurring during a TC are complex and interrelated than it appears. TCs' associated risk or damage assessment require detailed understanding of these complex interactions (Bruyère et al., 2019). These hazards are interlinked and have adverse effects on structures (buildings, power infrastructure, bridges), causing sometimes complete structural collapse (Czajkowski & Done, 2014; Pokhrel et al., 2021). Winds have significant direct or indirect impact on structures (natural/man-made) (OAS, 1991). For example, in deltaic island regions of Sundarbans, Bangladesh, combination of storm surge and wind led to embankment breach causing flood and inundation of low-lying regions (Mandal et al., 2022). Indirectly, in New Orleans winds led to overtopping of tress on a levee system, loosening the soil, thus increasing seepage and levee failure (Sanders, 2006). Forceful impact of flying debris (branches, wood, roofs etc.) due to wind has more impact than wind alone because these object can not only fall on people but also when airborne can blow into other structures or block roads (NOAA, 2023) causing secondary hazard events. Inland flood during heavy precipitation can not only cause problems inland, but when converged with storm surge and peak tide, threat to coastal areas intensifies (OAS, 1991). Various studies available assess the overall or combined impact of hazards during cyclone but lack in describing the interaction between these hazards (Bevacqua et al., 2023; Shen, et al., 2022; Nofal et al., 2023; Pilkington & Mahmoud, 2017).

To understand hazard interactions, it is evident to analyze the hazard during cyclone. One of the most prominent hazard is wind gust or high wind speed. Many winds models have been used for various purposes till date. In general there are three types of wind models - Parametric wind models (PWM), statistical models using machine learning (ML), numerical weather prediction (NWP) models, reduced atmospheric models (RAM) and Geographic Information Systems (GIS) based models. PWM are a type of physically based mathematical model includes simulation of wave, storm surge, wind structural design etc. of storms (Roldán et al., 2023) to predict cyclone wind field pattern. PWM when combined with hurricane track filed is capable of providing wind field data along the tracks (Chang et al., 2020). However, PWM is accurate in providing wind field pattern mostly around the eye, the zone of maximum wind speed. This model requires extensive data on wind: HRD Real-time Hurricane Wind Analysis System (H*wind) wind speed fields, boundary conditions (Roldán et al., 2023; Ruiz-Salcines et al., 2019), radial profile (Arthur, 2021) etc.

Statistical wind models using ML like wind generator (WINDGEN) have been used in measuring and predicting wind erosivity (Wagner, 2013). These deterministic models require hourly downscaling of wind

speed (Han et al., 2023). The applicability of the model is not studied for tropical cyclone setting. However, this technique can solve issue of unavailability of high resolution data by ML downscaling wind parameters using topographic characteristics at a mesoscale (Liu et al., 2023; Oh et al., 2022). ML have also been used (Chen et al., 2020; Wang et al., 2022) for cyclone trajectory and intensity prediction. Srinivas Kolukula & Murty, (2022) used ML to generate wind field during cyclones Fani and Thane with storm surge result computed from Advanced Circulation (ADCIRC) + Simulating Waves Nearshore (SWAN). Wu & Snaiki, (2022) and Mostafa et al., (2022) used wind parameters (speed, direction) and buildings characteristics to determine structural damage. In some works building characteristics have been extensively employed to get wind flow and pressure prediction at a local level resolution (BenMoshe et al., 2023; Y. Li, Huang, et al., 2022). For assessing building damage, convolutional Neural Network (CNN) has been successfully employed using post disaster images after Haiti earthquake (Nia & Mori, 2018). This requires ground-level building damage data for assessing damage from hazards without using hazard parameters.

Of the many NWP models, weather research and forecasting (WRF) models are used explicitly for their detailed resolution at mesoscale and variation in parameterization (Mi et al., 2023). Skamarock & Klemp, (2008) used WRF model for weather prediction after hurricane Katrina. Alimohammadi & Malakooti, (2018) and Nasrollahi et al., (2012) studied WRF parameter schemes for better prediction of cyclone Gonu and Hurricane Rita respectively. TC Maria was remodelled using WRF to investigate the evolution of the TC over time and its causes of intensification (Jury et al., 2019). Mi et al., (2023) states that precision of land use/cover can significantly affect model result, which is an inherent constraint for any mesoscale model. Also, results may vary considering different physical parameters and variation in topography input, which makes interpretation very unstable (Carvalho et al., 2012). WRF is combined with computational fluid dynamics (CFD) to get better results at microscale (Li et al., 2019). The data requirements for WRF is quite explicit since, besides topographic data, it requires physical parameterization and planetary boundary conditions (Li et al., 2021; Yu et al., 2022). It also requires humidity, surface data, soil and sea surface parameters as input data, making it quite extensive in computation (Carvalho et al., 2012; Tiesi et al., 2021; Yu et al., 2022).

Another type of NWP models is a simple fluid flow model like Reynolds-averaged Navier-Stokes (RANS) and large-eddy simulation (LES), which are also used at microscale for various purposes. Wind turbine performance assessment by Syawitri et al., (2021) used RANS-LES model for better flow features of wind turbines. Wind farm simulations also use the model which was able to capture the complex flow features around the boundary layers of the atmosphere (Adcock et al., 2022; Taghizadeh et al., 2015). RANS-LES was also used to simulate detailed wind flow in forests using LiDAR (Boudreault, 2015) and gas flow in cyclone (Jafari et al., 2017). Simplified version of this required wind speed data and Navier-stokes equation (Ebenhoch, 2015). However, this study is mostly used for wind farm simulations. RANS is also used in Computational Fluid Dynamics (CFD) models that are highly detailed and provide a high-resolution simulation of wind and waves, these models are capable of providing wind flow pattern around buildings and other structures (Tossas & Leonardi, 2013). In the paper by Mortezazadeh et al., 2022, a model had been proposed called CityFFD which is capable of simulating urban microclimate like wind velocity, temperature, local precipitation etc. It is stated to be advanced than CFD models being faster, and more detailed in providing accurate results for urban microclimate. For better simulations LES is incorporated to provide real-world simulation scenarios (Katal et al., 2019; Mortezazadeh et al., 2021).

In GIS-based models, building information modelling (BIM) is integrated to simulate community level 3-D wind hazard model using impact of wind pressure as the hazard parameter at a building level. However, the availability of detailed data for buildings might be impossible to obtain for many regions (Nofal et al.,

2022). Zeng et al., (2007) built a decision support system (DSS) that integrated forest growth model and wind damage model (HWIND) and embedded into GIS environment (ArcGIS) to assess wind risk damage on forest tress for Central Finland. DSS model was able to assess the number of tress and their dimensions vulnerable to critical wind speeds. The model gave both DSS and ArcGIS tools available to the users, but the computation was considered time consuming. URock is an open source GIS-based wind model designed specifically for urban environments. Like WRF, it requires surface data (soil, humidity), but computation is not complex. It requires building and vegetation layer for input as geographical data (Bernard et al., 2023).

For storm surge and landslide, several models have been employed. ADCIRC and SWAN was efficiently used for storm surge simulation (Silva-Araya et al., 2018; Srinivas Kolukula & Murty, 2022). Sea Lake and Overland Surges from Hurricanes (SLOSH) (Ell & Sprin, 1992) is being used by NOAA to diagnose the reaction of water to wind and pressure. Deft3D (Deltares, 2023) and SWAN (Manchia & Mulligan, 2022; Sapiega et al., 2023; Zhang et al., 2023) are open source models that is being used for generating waves, even for storm situations. HAZUS-MH is capable of modelling riverine and inland flood and also determine damage to buildings (Marvi, 2020). For landslides, Interferometric Synthetic Aperture Radar (InSAR) (Fobert et al., 2021) has been successfully used to increase quality of susceptibility maps for landslides in Dominica. ML can also be incorporated into landslide susceptibility analysis for obtaining relationship between landslide and environmental factors (Achu et al., 2023; Goyes-Peñafiel & Hernandez-Rojas, 2021; Q. Hu et al., 2020; Sun et al., 2021). Flood extent from storm surges and landslide susceptibilities and prediction has been studied and well analysed in many studies Mehravar et al., 2023; Islam et al., 2021; Wang et al., 2021).

However, all these hazard models for wind, storm surge and landslides, take each hazard as single hazard events or formulate an empirical equation for the relationship between the hazards and environmental parameters. These models fail to provide a segmented impact of each hazard and separate it from the following or cascading hazards.

Especially, looking at the islands in the Caribbean Sea, this cascading interaction of hazard events caused an enormous damage. Dominica, one the islands in Caribbean Sea had to withstand a long history of cyclones. Hurricane David (1979), Dean (2007), Frederick (2021), (Mohan, 2017), TC Erika (2015) and TC Maria (2017) (Dorst, 2021) are some of the catastrophic cyclones faced by this island. According to PDNA, (2017), for TC maria alone, total damage incurred was EC\$2.51 billion with housing sector taking the worst hit. This storm was severe to country's economy and social development, making TC maria event a focus of this study.

The interaction between the hazard events and its relation to multi-hazard risk during TC is one of the less studied arenas in hazard and risk assessment (Gill & Malamud, 2014). Considering a hazard phenomenon as a combined impact event, completely ignores the interaction between the various components of hazard. Theoretical attempts have been made for analysing the cascading nature of hazards during TC using hazard matrices (Gill & Malamud, 2016; Liu et al., 2016), stating primary hazard can lead to secondary and further trigger tertiary hazard. In 2016, a composite of hazard risk to landslide, earthquake, volcano, flood, storm surge and wind was made by USAID (Government of the Commonwealth of Dominica, 2016), that demarcated the whole island into four (very high, high, moderate, low and very low) levels of risk. However, quantitative analysis of the same on a higher-resolution capturing the interactions between hazards during TC event is scarce in research.

The sequence of hazard in a multi-hazard event and their complex interaction with each other is lacking in multi-hazard studies, hampering adequate risk assessment. Spatial and temporal extent of a hazard impact and its triggering effect for the secondary hazard is crucial to understand multi-hazard events. This study aims to fill this gap of understanding spatial and temporal sequence of hazard interaction and its linkage to associated damage using case-study regions in Dominica, Caribbean Islands, after TC Maria in 2017. For this study, CityFFD model was used to model wind, due to the unavailability of wind map for Dominica during TC Maria, this model was used to understand the wind patterns and its effects on buildings and structures.

1.2.   Research objectives

To analyse and model multi-hazard interaction between wind, storm surge and landslide processes on structures after TC Maria in Dominica.

Sub objectives:

1. To determine the types, dynamics and sequences of multi-hazard interactions based on forensic aerial and site-investigation of impact of TC Maria on Dominica:
    1.1.   What are the observed interactions between wind, landslide and flood processes during TC Maria?
    1.2.   How did the combined impact of the hazard interaction affect the infrastructure?
    1.3.   Which regions were the most affected during TC Maria by multi-hazards?

2. To determine the most suitable scale (city, building, or island etc.) and wind modelling approach for analyzing multi-hazard interactions after TC Maria:
    2.1.   What are the available wind models that have been used to represent local TC wind patterns?
    2.2.   What are the meteorological parameters to be included in the model that influence wind damage of buildings and infrastructure?
    2.3.   What is the quality of the wind model in providing localized and precise insight into building wind damage?

2. STUDY AREA

Situated in storm basin of North Atlantic, Dominica is located in a specific storm corridor called Main Development Region (Goldenberg & Shapiro, 1996) making it susceptible to tropical cyclones. Dominica is a small island in in the Lesser Antilles (Bryce et al., 2022). It is situated (15°25'N, 61°21'W) half-way in the middle of the island chain between Islands of Guadeloupe in the north and Martinique in the south (Figure 2). With a total area of 750 km², this island has a dimension of about 17 km in an east-west direction and 45 km in the north-south.
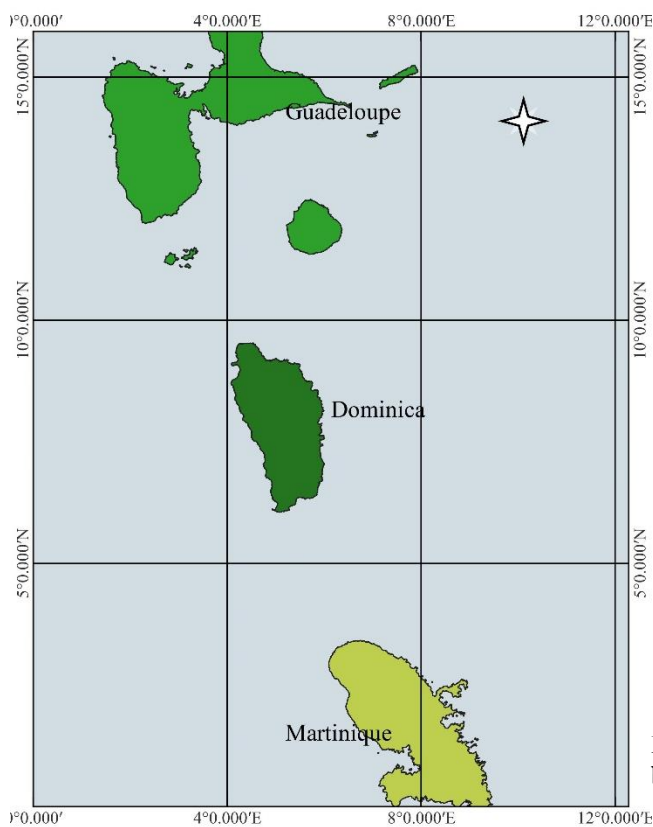
The island of Dominica consists of 7 volcanic peaks making Dominica the most mountainous island (Lindsay et al., 2003) compared to other Caribbean islands. Being in the humid tropical part of the world, eastern Dominica receives average 500 cm in eastern coast every year, and western 180 cm annually (Battut et al., 2023), which implies that there is spatial variability in receiving the amount of precipitation. The central island although it receives a huge amount of precipitation every year, the entire island is considered unsuitable for modern-day agriculture due to risk from sheet erosion and water stagnation (Barclay et al., 2019). Abundant precipitation has created a large network of over 350 streams, capable of carrying huge amounts of water posing vulnerability to flood due to overflowing during heavy rainfall or flash flood events.

Figure 2: Study area showing the position of Dominica between Guadeloupe and Martinique

Dominica is known to have a rugged terrain due to its volcanic origin (Howe et al., 2014) making it susceptible to landslides during heavy rainfall events. Being a mountainous region, flood water and wind gusts brings debris, vegetation load and huge boulders downstream (Schaefer et al., 2020). Fine, permeable soil increases the risk of water erosion (Battut et al., 2023) which ultimately leads to landslides. The occurrence of landslides and heavy mass movement disrupts communication, transportation thus also evacuation, agriculture and infrastructure of the island. Soil characteristics along with vulnerability to extreme weather events like cyclones and flood have caused huge catastrophes in this island (Battut et al., 2023). Historical cyclones dates back to Great Hurricane in 1780s. In the recent years TC David, Dean, Erika and Maria in 1979, 2007, 2015 and 2017 respectively have disrupted the entire natural and societal system of Dominica. TC Maria triggered around 9900 landslides causing total damage of 930.9 million USD, damaging transportation and agriculture and housing facilities (Fobert et al., 2021).

Figure 3 shows the number of storms and hurricanes between 1950 and 2019. The last decade 2010-2019 saw the most number of storms (Battut et al., 2023). Legend 1 represents the unnamed and tropical cyclones, 2 is associated with category 1 and 2 tropical storms and 3 are the major TC. The graph represents the vulnerability due to the presence of numerous cyclones each decade.
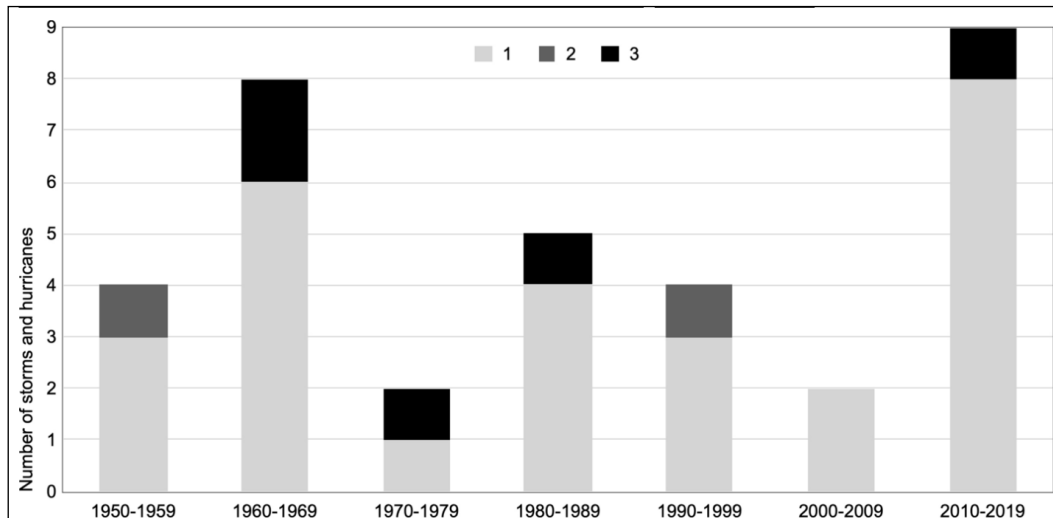
Figure 3: Frequency of cyclone between 1950-2019 passing 2100 km or less of Dominica

With the occurrence of multiple hazards from flash flood to volcanoes and cyclones, the economic system on the island-nation have severely affected from 1700s (BBC, 2017). Reduced employment forced people to settle on the outer edges of big cities like Roseau and Portsmouth. Houses are built mainly in the low-lying fluvial flood plains which are explicitly prone to hydrometeorological hazard events (Battut et al., 2023). From the governments also there was negligence in investment for networks and residence building to withstand the natural hazards (Barclay et al., 2019). Isolation and poor inhabitation increased the vulnerability of these low-income group people to hazards (Barclay et al., 2019). It has been recently taken into consideration to invest in hazard resistant buildings in these regions by the government. Due to the vulnerable nature of this island to TCs, many international organizations have taken initiative to strengthen resilience and recovery of the island. United Nations Development Programme (UNDP) have launched Climate Resilience and Recovery Plan (CRRP) collaborating with Dominican Office of Disaster Management. United Kingdom and UNDP monitor the development of Climate Resilience and Recovery Plan (CREAD) in Dominica. Reduction of carbon was also aimed in Low Carbon Development Path (LCDP) project partnering with Japan to facilitate suage of low-carbon emitting technologies (UNDP).

One of the ongoing projects funded by European Space Agency (ESA) is EO4MULTIHA which focuses on the potential of Earth Observation tools to understand and analyze multi-hazard evens. It includes perception of risk, vulnerability and associated impact on the society. One of the research arena for this project is understanding the spatial and temporal variability of natural hazards using remote sensing data and statistical approaches. Dominica is one of the areas hit rampantly by hazard and thus my thesis work completely aligns with the ongoing EO4MULTIHA project. With the outcome of this work, the study can illustrate the interaction of wind, storm surge and landslide processes (hazard criterion) associated with the extreme weather events.
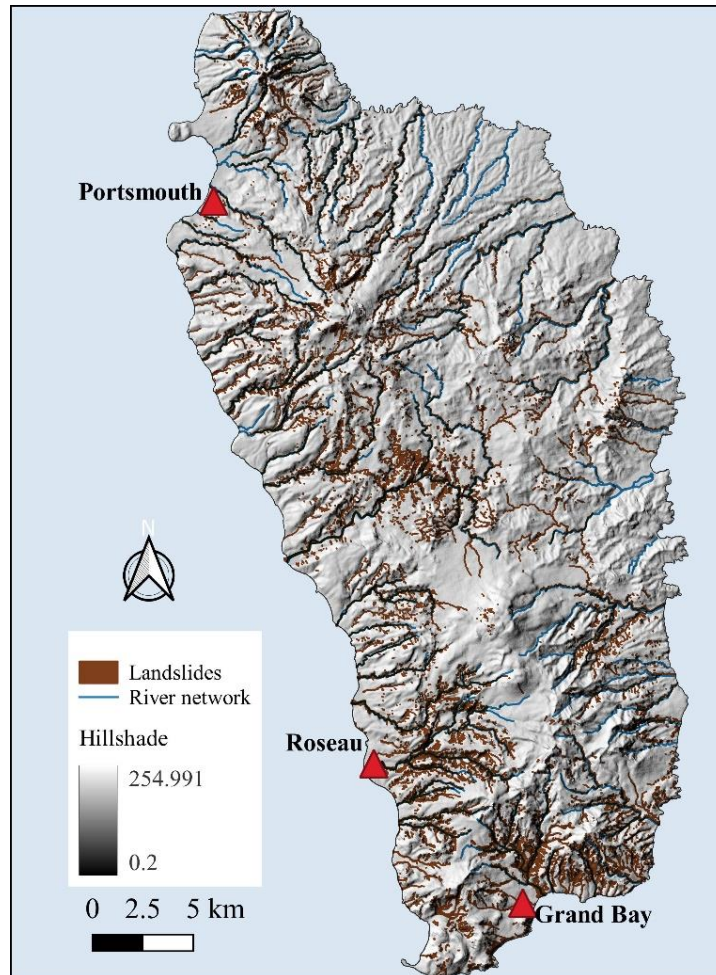
Figure 4: Dominica map showing case-study regions in red

The inventory map, Figure 4 made from the layers obtained from UNDP datasets, is a combination of flow processes that were visible later on satellite imagery, so also debris floods and some flood regions.

In order to assess the effect of multi-hazard on Dominica during one of the most prominent tropical cyclone events like TC Maria, three case-study regions (marked in red in Figure 4) are selected which are explain in section 5.2: Roseau, Grand Bay and Portsmouth, all situated on the western coast of the island. Roseau being the capital city of the island, has one of the highest density of population and infrastructural facilities (Barclay et al., 2019). Roseau consists of 21% of the population according to census 2011, followed by Portsmouth and Grand Bay. The capital city and Portsmouth are the most populated regions of the island as they are the most urbanized centres. Roseau along with Portsmouth are considered the hub of fishing activities and operations in the western coast (Guiste et al., 1996).

3. DATASETS AND SOURCES

The datasets used in this study are listed in Table 1. It is divided into two sections, one contains vector and raster datasets, while the other contains specifically meteorological data used for objective 2 i.e., modeling patterns of wind around buildings and other structures to understand the effect on wind on infrastructure during TCs.

Table 1: Datasets used for objective 1 and 2 along with sources, format and resolution

Dataset	Source	Data type	Year & state	Resolution	Objective	State
Drone data	Open Aerial Image[1]	Raster	2017-2018	3 – 5 cm	1	Static
Building damage characteristics	UMDP dataset	Tabular	2017-2018		1	
Digital terrain model (DTM)	UNDP dataset	Raster		0.5 m	2	
Digital surface model (DSM)	UNDP dataset (LiDAR data)	Raster		0.5 m	2	
Building footprint	Building inventory from UNDP	Vector	2017-2018		2	
Mesh file	CFD0 code editor	Gridded cells			2	
Meteorological data						
Global horizontal irradiance (GHI)	Global Solar Atlas	.png/.jpeg	1992-2018		2	Dynamic
u and v components of wind	EMCWF (ERA5-LAND)	Tabular	14th Sep-29th Sep 2017	11 km	2	
Air temperature	EMCWF	Tabular		11 km	2	
Dewpoint temperature	EMCWF	Tabular		11 km	2	
Relative humidity	Derivative from ERA5-LAND	Tabular		11 km	2	

3.1. Drone Image

Drone data was collected from an open source database. It consists of dates ranging from September 2017 to January 2018. This date range gives a good idea of immediate hazard effects on 2017 and preliminary mitigation strategies like temporary roof covers later in November 2017 and early 2018. The drone images cover specific parts of the island like Roseau, Portsmouth, Coulibistrie, Salisbury, Dublanc, Point Michel, Savanne Paille in the western coast, Pichelin in the central part, Pointe Mulatre, Boetica, Laplaine, Kalinago and Marigot on the eastern side of the island. Organizations like GlobalMedic ran program called RescUAV to take drone shots after the hazard. They operate by sending Canadian volunteers throughout the globe to provide search and rescue operations after any hazard. The drone images are taken by these volunteers after TC Maria to understand the hazard effects that occurred. See Table 1 for the source.

---

[1] OpenAerialMap Browser

According to Womble et al., (2005), (2006), satellite images with 0.6–1.0 m resolution are demonstrated to give information on roof structure damage, removal of a chunk of building from wind damage etc. Since the obtained dataset consisted of average 4 cm resolution UAV image, it was used for inspecting visual damage detection.

3.2. Building characteristics (UNDP dataset)

The collection period of this data ranges from 26th October 2017 to 29th January 2018. 29432 houses were surveyed and recorded with all building information and post-disaster damage assessment (see section 11 appendix) for data column information. This dataset was collected from ITC Applied Earth Science (AES) department since it was not publicly available. The UNDP project data comprised of fractional damage to the majority of buildings, and their structural elements (roofs, floors, walls, ceilings) for the island along with elevation datasets. Also, the damage data per building (geolocated) after the cyclone was not publicly available. An illustrative .csv file containing the location as well as associated information of all the houses in Dominica were collected by UNDP.

3.3. Digital surface model (DSM) and Digital Terrain Model (DTM)

DSM using Light Detection And Ranging of Laser Imaging Detection And Ranging (LiDAR) was collected after TC Maria in Dominica. It covered the whole of Dominica at 0.5 meter (m) resolution. DTM with 0.5 meter resolution also collected during UNDP project, did not cover the inner region of the island, however, all 3 case-study regions are coastal regions which were well covered by this data layer. See Table 1 for its usage.

3.4. ERA5-LAND

ERA5-LAND is known to provide a consistent data of the evolving land compared to ERA5 at a higher resolution. Reanalysis dataset combines the modelled data with the observational or real world data to produce a complete and continuous dataset cohering to the laws of physics. Unlike its previous version ERA-Interim, Era5 combines new observations improving the observed climate parameters, enhancing the temporal and horizontal resolution. ERA5-LAND is produced by ECMWF land surface model: Carbon Hydrology-Tiled ECMWF Scheme for Surface Exchanges (Muñoz-Sabater et al., 2021). It covers a period starting from January 1950 till 2-3 months prior to the present representing water and energy cycles. The same temporal resolution is maintained as ERA5, but with higher spatial resolution 0.1° * 0.1° (Bonshoms et al., 2022). Its native horizontal resolution is from 9 km grid spacing via linear interpolation with a vertical resolution from 2 m above the ground surface.

ERA5-Land model utilizes atmospheric variables from ERA5, such as air temperature and humidity, as input data to regulate and constrain the simulated land surface conditions, called atmospheric forcing. This process plays a crucial role in keeping the ERA5-Land model's estimates grounded in reality by continuously adjusting the simulated land fields based on observed atmospheric conditions. However, the quality and quantity of these observational data used for atmospheric forcing diminish as we go back in time, leading to a growth in the uncertainty of the model estimates for earlier periods. Thus, ERA5-LAND datasets provide to certain extent uncertain information.

3.4.1. U and V components of wind

As an input for the wind model, ECMWF Copernicus ERA5-LAND hourly data was used. For u and v components of wind, the vertical component (v) is obtained from 10 m above the ground surface (Muñoz, 2019).

According to Gualtieri, (2021) and Potisomporn et al., (2023) ERA5 reanalysis products cover inaccessible regions and even offshore sites, well capable of predicting wind speed. Thus having large spatial resolution, ERA5-LAND products are capable for flood and drought forecasting (Muñoz, 2019). For this study hourly data was used since wind speed can change very frequently during extreme events like TC Maria. U component of wind correlates to the horizonal or westward movement of wind at 10 m height from ground, computed in meters per second. Similarly V component of wind also has the same unit but is the northward direction of wind from a 10 m height above the ground (Muñoz, 2019). It is an open source freely available wind dataset from Copernicus.

3.4.2. Dewpoint, Air temperature and Relative humidity

Both dewpoint and air temperatures are captured at a 2 m distance from the surface of the Earth and are measured in Kelvin. These two temperatures were used to calculate the relative humidity due to lack of relative humidity in ERA5-LAND dataset. Relative humidity is the "amount of actual water vapor pressure to equilibrium vapor pressure" known as "saturation vapor pressure" (Lawrence, 2005). The equation by Lawrence, (2005):

$$RH = 100 - 5 * (T - Td)$$

where T is air temperature at 2 m and Td is dew point temperature at 2 m.

3.4.3. Global Horizontal Irradiance

This value estimates the overall solar power (in kWh/m³) available for electrical power generation. It is the average daily/yearly sum of GHI from 1999-2018 spanning over 20 years. Solargis model from atmospheric and satellite data with a time-step of 30 minutes is used for the calculation of this value. It is an initiative taken and published by World bank 2019. It is an open-data source which can be downloaded from here. It spatial resolution is 250 m which is very coarse compared to DTM and DSM, hence, is seen to be relatively uniform for the case-study regions. ERA5-LAND did not contain this specific information on GHI, hence, an alternative source was obtained. This dataset is part of the meteorological data mentioned in section 4.2.

4. WIND MODEL: CITYFFD

City Fast Fluid Dynamics tool (Mortezazadeh et al., 2022) developed Concordia University is a 3Dimensional Fast Fluid Dynamics. It was developed for the production/simulation of local wind simulations. Compring with other CFD model, this uses higher order semi-Langrangian equations, leveraging power of Graphics Processing unit (GPU). The model is aimed to model flow of air, pollution and temperature distribution in the urban environments. Non-dimensional Navier-Stokes equations (Katal et al., 2019):

$$\partial u_i / \partial x_i = 0$$
$$\partial u_i / \partial t + u_j \partial u_i / \partial x_j = -(1 / \rho) \partial p / \partial x_i + \nu \partial^2 u_i / \partial x_j^2 + g_i \beta (T - T_0)$$
$$\partial T / \partial t + u_j \partial T / \partial x_j = \alpha \partial^2 T / \partial x_j^2$$

where, u_i represents the velocity components,
x_i represents the spatial coordinates,
p is the pressure,
ρ is the density,
ν is the kinematic viscosity,

gi is the gravitational acceleration,

β is the thermal expansion coefficient,

T is the temperature,

T_0 is a reference temperature and

α is the thermal diffusivity.

CityFFD can be divided into two modelling steps: preprocessing or data preparation and model simulation (Figure 5). Data preparation includes geometrical data, weather data, specific building and archetype dataset (Mortezazadeh et al., 2022). This step includes data collection, cleaning and assembling datasets to be provided as input for the model.

4.1.   Geometrical data

This dataset includes building footprint, height, window-wall ratio, orientation kind of occupancy etc. Non-geometrical data includes the type and year of construction. When considering urban regions geographical information like the terrain can also be integrated not this model (Mortezazadeh et al., 2022). Originally archetype data consisting of building shape as part of an extension of CityFFD model, called CityBEM. This extension concerns with thermal aspect or temperature variation in urban simulations (Mortezazadeh et al., 2022). This study focuses on wind patterns and in-built temperature variations and not with CityBEM which models urban microclimate temperature patterns. Urban microclimate not being a part of his study, CityBEM was switched off.
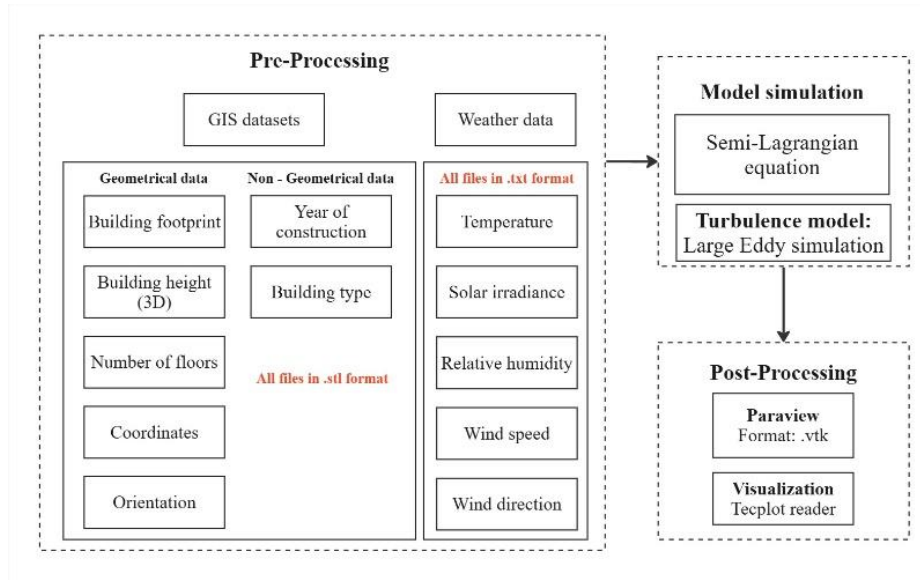
Figure 5: Steps for wind simulation using CityFFD

4.2.   Meteorological data

Hourly data (0:00-23:00) for a date range of 14th – 25th September 2017 was used in this study. This date range was used to collect all ERA5-LAND datasets. According to the research article Bruneau et al., (2024), it is suggested to use a time frame that captures the cyclone's stages of evolution and dissipation. Specifically, the paper recommends using a time frame from a few days before cyclone formation to a day or two after dissipation. TC Maria was deemed a tropical depression on 16th September marking its initial stage and started to dissipate from 20th September over Domnica (Manikanta et al., 2023; Pasch et al.,

2023). Hence, a time frame from 14th September to 25th September is used to ensure sufficient data capture from TC Maria's evolution, to weakening phase, which are crucial for accurate wind modeling.

The input of weather dataset includes hourly measurements of u and v wind components, dew point and air temperature, relative humidity, GHI (Please refer section to 3.4 for data description), wind direction and wind speed calculated from u and v components of wind (refer to section 5.4.1 for details).

4.3. Result visualization

CityFFD output are generated in .vtk files which can be visualized in tools like paraview using Tecplot reader (Katal et al., 2019). The file format consists of file version, header, file format (here ASCII), data structure and data values. U and V components of wind average values are recorded in this .vtk file format.

5. METHDODOLOGY

5.1.   Damage interpretation

To determine the types of hazard effects and their interactions like blown roof, blocked drainage, uprooted trees, it is important to analyze the direct & indirect effects of hazard events, human activities that might have caused or aggravated the hazard impacts. Analysis of pre and post images allows for pinpointing the types of impacts that occurred. Objective 1 was achieved using visual inspection from high resolution UAV images and from field survey data collection (section 6). High resolution drone images were used for preliminary visual inspection of post-disaster damage. To have an initial estimation of the general damage pattern visual inspection have been considered a good starting platform (Lozano & Tien, 2023). For this study the approach by Ghosh, 2010 was adopted, explains precisely the methods for visual inspection of damaged buildings after an earthquake.

The damage interpretation was done comparing pre-disaster images on Google earth Pro (2014 & 2015) and post-disaster drone images using steps similar to Ghosh, 2010:

1. Review all the buildings falling within case-study regions
2. Identify and point-digitize collapse/damaged buildings pertaining to wind, flood: Blocked drainage was attributed to sediments brought down by streams during flood. Blown/no roof shade or roofs with blue temporary covers were associated with roof damage by wind. In Figure 6a, houses were seen to be completely destroyed without any standing structure. Completely destroyed state was associated to wind and flood damage. If the roof was blown but structure still stood and floor is intact with furniture placed inside (Figure 6d), the damage was associated to wind.
3. Flood identification: Debris brought down by streams block drains and bridges shown in Figure 6c causing more flood due to slow passage of water. The blockage of bridges and roads are attributed to flood events.
4. Landslide identification: landslide shapefile from UNDP dataset was overlayed on Google Earth images and drone images to compare which region was impacted by landslide (see Figure 6b). Right image shows the spots highlighted in red for landslide which are covered with trees in left image, pre-disaster in 2014.
5. Make separate layers for each hazard damage and color code for each hazard type.

Figure 6: Damage interpretation: a. Houses completely destroyed after Maria in Roseau; b. Occurrence of landslides, Roseau; c. Blockage of bridge by debris brought downstream by rivers; d. Left image shows houses pre-disaster; right image shows roofs blown with interior of buildings still intact with belongings. Blue covers/tarps are the temporary shades provided after TC Maria

Presence of temporary roof covers in post-disaster images after cyclone Maria might have hindered this analysis (Womble et al., 2010). With only nadir/top of buildings views available for the drone images, low-

level damages might have been overlooked during this analysis. This preliminary inspection of damage images was used for field survey guidance and corroborating other sources in selecting case-study regions for field work.

5.2.   Forensic field investigation

Field visit or forensic field investigation was conducted to understand root causes of disasters, outlining dynamic risk chains, analyzing direct and indirect impacts, determining timeline or sequence of hazards etc. (Atun, 2023). For the purpose of understanding objective 1, field survey was conducted in Dominica over 7 days and data was collected from 12th to 18th February 2024.

Case-study regions for field visit within Dominica were chosen depending on PDNA damage report, UNDP damage classification along with damage interpretation using drone image (see section 6.3). According to PDNA, 2017, certain regions were heavily affected more than others during TC Maria: Airport of Roseau i.e., Douglas Charles and Portsmouth airport, were reported as severely damaged. Washouts were reported to occur from Loubiere to Grand Bay which was one of the primary care center during Hurricane David. Huge structural damage of major bridges and roads occurred after the disaster in Roseau (PDNA, 2017b). Combined hazard map from (Government of the Commonwealth of Dominica, 2016) demarcated western coast regions at higher risk compared to eastern coast. Besides post-disaster assessment records, other factors like terrain difference was also taken into account. Areas that differ in topography (determined from DTM) were selected to understand presence of topography effect during interaction of hazard (if any). Due to the extent of damage after TC Maria and topographic difference analysis between different case-studies, three regions: Roseau, Grand Bay and Portsmouth were, selected for field survey.

One-to-one interview were conducted in subsection of households in the chosen case-study regions. The choice of household to be visited was based on UNDP impact assessment dataset acquired from the AES department, ITC containing damage level information explained in the later section. Research study using personal interviews have been conducted to collect post-disaster information from people of Dominica after storm events by UNDP (unpublished) after TC maria, where extensive personal survey had been done. The results from UNDP survey were used to select the places to be visited during field survey in Dominica for all the three case-study regions. Damage percentage was extracted from UNDP excel sheet and used for selection of households to be visited (Table 2).

Table 2: Shortlisted data of damage classification

	Roofs	Walls	Floor	Ceiling	Classification
Damage levels	Less than 24%	Less than 24%	Less than 24%	Less than 24%	Very low
	Between 25% and 49%	Between 25% and 49%	Between 25% and 49%	Between 25% and 49%	low
	Between 50% and 74%	Between 50% and 74%	Between 50% and 74%	Between 50% and 74%	medium
	More than 75%	More than 75%	More than 75%	More than 75%	high

Houses with damage level more than 75% (high) were shortlisted. From this list, only high damage of floors, roofs, ceiling and walls were used to coordinate the houses to be visited. The reason behind this

selection was done based on certain assumption ideas: floor damage corresponds to landslide or flood effect (Bodoque et al., 2016; Brencich, 2010; Luino et al., 2009) and roof damage by wind. Studies discuss that loss of envelope, sheathing, structure of roofs are mostly occurred due to wind pressure (Lee & Rosowsky, 2005; Singh et al., 2021; Sparks et al., 1994). Hence, by selecting houses with more than 75% of floor and roof damage, it might corroborate to higher damage by flood and wind respectively. The locations (Figure 7) were overlayed on top of Google Earth images to pin point the locations during field visit.

Figure 7: Overlay of GPS points for more than 75% damage for roofs in Roseau

Prior to the field visit, a list of questions related to hazard information, timeline of hazards and impacts were prepared and is shown in section 12 appendix. Apart from that, QR codes (60) were printed to be distributed in houses in case of no residents during the time of visit. Consent papers were also printed for ethical purposes.

The field survey was conducted by 3 people (including myself) from 12th February 2024 to 18th February 2024. The schedule and the itinerary of the field visit is shown in section 13 appendix. Two methods: 1. direct interview with citizens and 2. government officials were undertaken for obtaining information related to TC Maria and its impacts. During the interviews, citizens and officials (Table 3) were either shown the consent papers to asked permission to record the discussion using recorder. Answers were either recorded or written down for further analysis. The sample size of the survey was 20 combining all the three case study regions.

Table 3: Statistics of government official people interviewed

Meeting at Red Cross Division Roseau	1
Meeting at CREAD	1
Meeting w/ Office of Disaster Management	2
Meeting w/ Planning Department	2
Meeting w/ Public works	1

5.3.   Impact chain methodology:

After the completion of damage interpretation and forensic field investigation, hazard location maps were made which showed the presence of hazards during TC Maria in specific regions of Dominica (See Figure 10). To visualize the various hazards present during the cyclone, impact chains were made which showed

the process and effect of each hazard and how they combined to cause a multi-hazard reaction chain. According to Menk et al., (2022), impact-chains are a blend of surveyed, quantitative or measured data. For this research work, the chains were based on field survey data, satellite imagery, drone surveys and literature review. The guiding questions from Hagenlocher et al., (2018) was explicitly used for the purpose of making this impact chain:

1. Identify the climatic hazard: TC Maria, 2017
2. Identify the required climatic signals which caused impacts or increased risk: here heavy precipitation and high wind gusts
3. Identify the intermediate impacts and risks: here soil moisture and slope leading to secondary hazard generation.
4. Determine the exposed elements to risks in the socio-ecological system: here natural vegetation, infrastructure and society.

Three impact chains were developed for the case-study regions of Roseau, Portsmouth, and Grand Bay. The separation of these hazard chains enables a detailed delineation of specific hazards impacting each region, facilitating the identification of differences in hazard combinations. The primary data sources for this analysis included field investigations and interviews with government officials. PDNA, 2017 was used to validate the information.

To address Question 1, the Post-Disaster Needs Assessment was referenced, providing a comprehensive description of the climatic hazards that devastated Dominica in 2017. Further insights into the formation of Tropical Cyclone Maria were derived from Hurricane Maria: Hydro-Meteorological Impact on Dominica, (2017); Pasch et al., (2023). Question 2 was investigated through field survey results, wherein the public identified the initial climatic hazard that occurred first and precipitated subsequent impacts. The distinction between primary and secondary hazards was effectively analyzed using the frameworks provided by De Angeli et al., (2022); B. Liu et al., (2016), and van Westen et al., (2014). These studies elucidated the mechanisms behind the causes for secondary hazard generation. Local factors, such as topography and soil characteristics, were identified by government officials during field surveys as significant contributors to secondary hazards in the case-study regions, addressing Question 3. The final question pertained to the exposed elements of risk, categorized into physical (infrastructure), social, and economic sectors. This categorization aligns with Monge et al., (2022), who identified these sectors as the primary areas affected during cascading events. According to Browne, (2020), health, housing and natural ecosystem also was affected by TC Maria. Hence, they were also highlighted in impact chain. Impact on Trees, cropland were assigned to "impact on natural system'; destruction of buildings, bridges and other infrastructure were attributed to "impact on infrastructure" and hindrance to food and evacuation needs during and after TC Maria was categorized under "socio-economic impact".

5.4. Wind model: CityFFD

As mentioned in the introduction, wind is one of the prominent hazards that occur during tropical cyclone. To understand the hazard interactions in selected case-study regions, wind modeling was performed. Without any prior wind map available for Dominica to analyse the hazard interaction, wind model was simulated to assess the impact of wind on the case-study regions.

One of the objective was to analyze the available wind models, their capabilities concerning scale and spatio-temporal dimensions of the multi-hazard interactions on Dominica and select the best suitable one to analyse hazard interaction for the purpose of this study. The criterions used were less computational load, faster computation, able to capture topographic effect, able to capture multi temporal scales, and also

is feasible to run within the timeline of this study. Several literatures mentioned in section 1.1 was referred to choose the suitable wind model that is capable of capturing terrain or topographic effect of wind (if any) in case-study regions. Upon research, CityFFD (Mortezazadeh et al., 2022) was selected as the wind model to be used for this study. The primary focus was to analyze the effect of topography on wind speed and highlight areas of high and low wind speed, assuming that most damage was reported.

To understand the topography effect on wind patterns between the chosen case-study regions, topography was introduced in this wind model. However, due to resource limitations concerning computational requirements mentioned in section 8, another simulation was performed without topography. Hence, the methodology for wind model includes two sets of simulation with and without topography.

5.4.1. Wind model without topography

Preprocessing:

Wind simulation was performed without the effect of topography from CityFFD web portal (Mortezazadeh et al., 2022). The process initiates with the generation of geometry (.stl) file. Figure 8 shows the area simulated for CityFFD without topography in red building footprint. The raster (.tiff/GeoTIFF) difference of DSM and DTM was calculated to obtain the building height without terrain (red box in Figure 9). The building raster height .tiff layer was converted to vector (.shp) file with 'height' column corresponding to building heights. The .shp file was then exported to .geojson file to directly import into CityFFD portal. This web portal automatically exports .stl file using 'height' column to produce 3D objects. Autodesk Netfabb inbuilt repair script was used to quickly repair discontinuities and surface (see Figure 8). STL files generally contain errors due to the process of mesh conversion like gaps, holes, overlapping triangles, and poor mesh quality, which can lead to inaccurate or unstable simulation results. Repairing mesh ensures a watertight geometry, improves mesh quality, simplifies complex mesh.

Initial extent of the simulation region was of green bounding box in figure 8, but while importing Geojson file into CityFFD portal, the web portal crashed and hence, present extent was used.
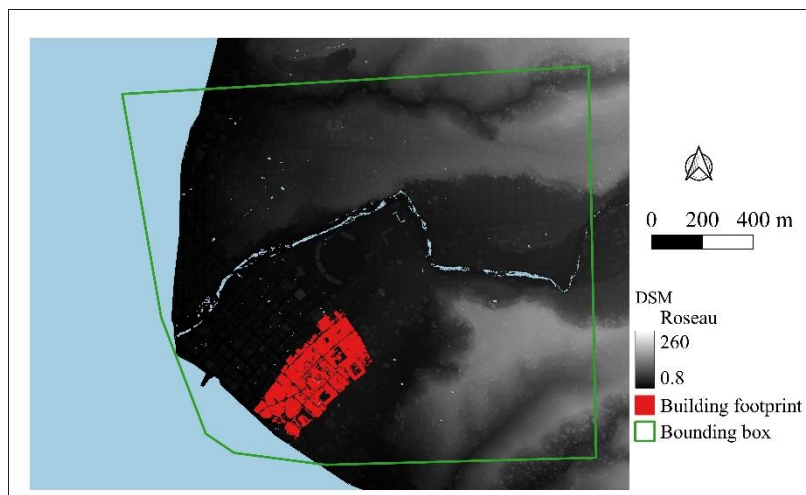
Figure 8: Roseau regions simulated for wind model

The dimensions of the produced .stl file was used to calculate a domain or bounding box. The size of the domain file was determined using the formulae proposed by Wang et al., (2023). The minimum vertical length of the domain: $5H_{max}$ where H_{max}= tallest building height. The lateral dimensions were H_{max}. The maximum building height in the geometry file being 26 m, dimensions of the bounding box (domain) was chosen as 2 km long, 120 m high and 1.2 wide (Table 4). All calculations for the domain were made after

consultation from study by Wang et al., (2023). A uniform mesh was generated of resolution 5 m using CFD0 code editor. The resolution of the mesh file was 5 m spacing since the geometry file was generated using 0.5 m resolution DSM and DTM capturing detailed surface objects. Figure 9 explains steps taken for this approach.

For the weather data, wind speed and direction were calculated using the formulas in excel file for all the dates at an hourly basis suing the following formulae:

$$Wind\ speed = sqrt(u^2 + v^2)$$
$$Wind\ direction = atan2(v, u)$$

The application of the formulas are valid as shown in study by Hersbach et al., (2020). The excel sheet also consisted of hourly air, dew point and ground temperature, and relative humidity.
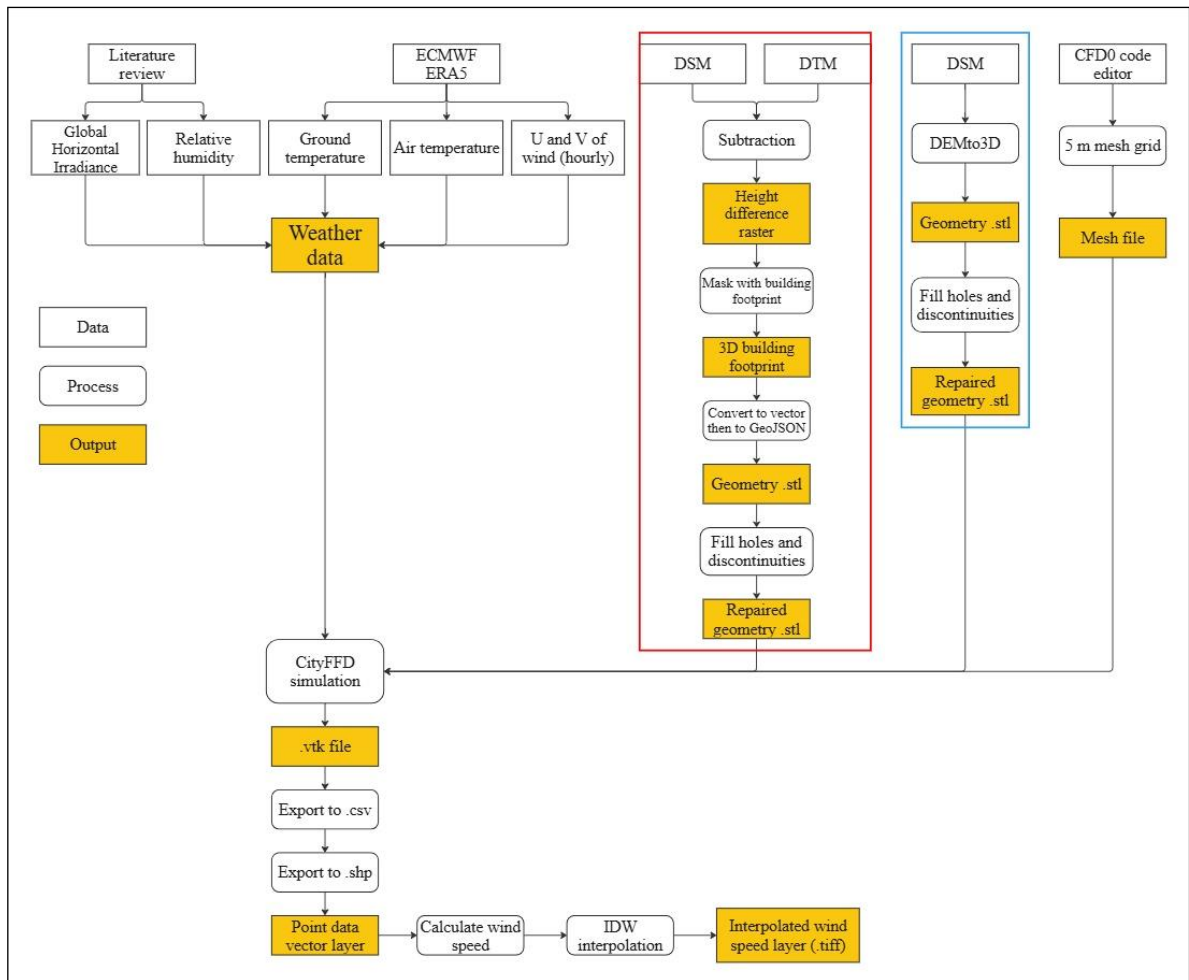
Figure 9: Wind model methodology flowchart

Post-processing

Following a simulation time of approximately one hour on a laptop, the outputs were generated in VTK files. These results were visualized using Tecplot reader in ParaView. Given that ParaView does not support .shp or .tif files, the VTK files were exported to .csv format for further analysis. The data was imported into QGIS, considering only x and z coordinates, while omitting the y-axis (height of buildings). A new column, labeled 'wind,' was created to calculate wind speed using previously established formulas.

To maintain interpolation resolution consistent with the grid resolution, Inverse Distance Weighting (IDW) interpolation was applied with a 5-meter spacing on the wind column. According to W,u et al.,

(2016),IDW is a computationally efficient and straightforward interpolation method, especially advantageous for quick analyses. This method is effective in capturing local variations in climatic variables such as precipitation and temperature. Given that this study focused on the meteorological variable of wind, which involves significant local variations, IDW interpolation was deemed the most suitable choice. The resulting output is a point data layer of interpolated wind speeds for the selected area (see Section 6.4). This point data layer was subsequently exported to .tiff format for enhanced data visualization.

Visualization
Depending on the maximum height of y-axis, the slicing for the wind speed calculation was made at 6 m at y-axis in paraview. The formulae collected from University of Concordia was used to calculate wind speed in paraview.

$$ihat * u\_AVE + jhat * w\_AVE + khat * v\_AVE,$$

where,
ihat/jhat/khat = constant value
u_AVE = time-averaged u component of wind (m/s)
w_AVE = time-averaged w component of wind (m/s)
v_AVE = time-averaged v component of wind (m/s) (height factor)
Overlay of wind speed map section 14 appendix was attempted with buildings footprint shown in red in Figure 8.

Validation
The results of the damage interpretation through visual inspection (see section 6.3) are used to be validated against the results from wind model although, the results of the wind model without topography does not reflect the wind patterns in reality.

5.4.2. Wind model with topography
The initial plan for this segment was to combine .stl fie for buildings and .stl file for terrain in an external application like blender and get .stl file combining building overlapping terrain. However, due to computational limitations associated with combination of hardware and used softwares, idea of using separate building and terrain layer was rejected.
DSM was used as a representation of both building and terrain since 0.5 m resolution had high surface details including building, tress etc. For this simulation the bounding box marked in green in figure 8 is used. The extent of this box captures the two ridges present in Roseau, which was expected to cause topographic effects by shielding buildings from high wind gusts.
To generate .stl geometry file, in this simulation, only DSM was used. Figure 9 highlights the process of .stl file generation in blue box. The dimensions of the generated .stl file was used to calculate the bounding box size using the approach from Wang et al., 2023.The maximum terrain height was 163 m for highlighted region in green in Figure 8, so the domain size was 3 km long, 3 km broad and 600 m in height (Table 4).

Visualization & validation
Wind speed slicing was done at y-axis at a height of 20 m since the structures in the region are maximum 19-20 m. Results show that the model was unable to include topography in the simulation process, (see section 6.5), for which the validation of the model result was not progressed further.

Table 4 shows the dimensions of .stl geometry file and the boundary box for both with and without topography. The dimensions are calculated from Wang et al., 2023. It is to be noted that for CityFFD y-

axis is the height of the terrain or building and not z-axis. Hence, y minimum and y maximum represent minimum and maximum building height for section 5.4.1 and lowest and highest elevation surface elevation for section 5.4.2. This changes the orientation of the results after simulating in CtyFFD making comparison between reality and model result unreliable. Change in model result orientation changes the wind direction during TC Maria in reality (section 6.5 validation).

Table 4: Domain and geometry file dimensions

| .stl with terrain (Roseau)		
	Geometry (m)	Domain (m)
xmin	0	-500
xmax	1630	2500
ymin	0	-100
ymax	164	500
zmin	0	-500
zmax	1490	2500
.stl without terrain (Roseau)		
	Geometry (m)	Domain (m)
xmin	-440	-1000
xmax	480	1000
ymin	0	-20
ymax	26	100
zmin	-86	-500
zmax	218	700

Due to lack of computational capacity from the personal workstation during study, the wind simulation was limited to only the chosen section in Roseau as shown in Figure 8. Portsmouth and Grand Bay were not simulated due to lack of computational limitations.

6.   RESULTS

The chapter is compiled using the information collected during field visit from government officials and citizens. This section initiates with a map showing the overview of hazards that affected different regions of the island, Dominica during TC Maria. The map in Figure 10 will address the research questions like what are hazards that took place during TC Maria and if there was any spatial difference between the hazards taking place across the country. Furthermore, the impact chain for the whole island in general and then impact chain for case-study regions separately. The impact chain shows the impacts occurred due to hazard interaction and prominent hazards (highlighted in each impact chain) for the case-study regions. All the information shown here is recorded from government officials and citizens during one-one discussion in field investigation. The results from the interviews during fired investigation are shown as figure 10 and impact chains. For the validation of the results from interviews, PDNA and Domnica meteorological impact analysis was utilized. Also, damage response report after TC Maria published by International Federation of the Red Cross was reviewed.

6.1.   Oveview of hazards in certain areas of Dominica

The presence of various hazards and combinations in different parishes of Dominica were obtained. Figure 10 shows mainly 5 different kinds of hazards that were collected from interviews from the citizens and government organizations during field investigation. There is prominent difference in the presence of hazards spatially. The west coast is indicated to be more prone to rockfalls whereas the right coast is susceptible to landslides due to the presence of gentle slopes. These observations were specifically mentioned during the discussion with CREAD and Red Cross. Places like Dublanc in the north had rockfall while eastern coastal places like Petite Soufriere and Petite Savanne experienced prominent landslide episodes due to high and prolonged precipitation. Storm surge can also be seen in any parts of the island namely Grand Bay, Roseau, Scotts Head etc.

Figure 10: Areas with higher density of specified hazards
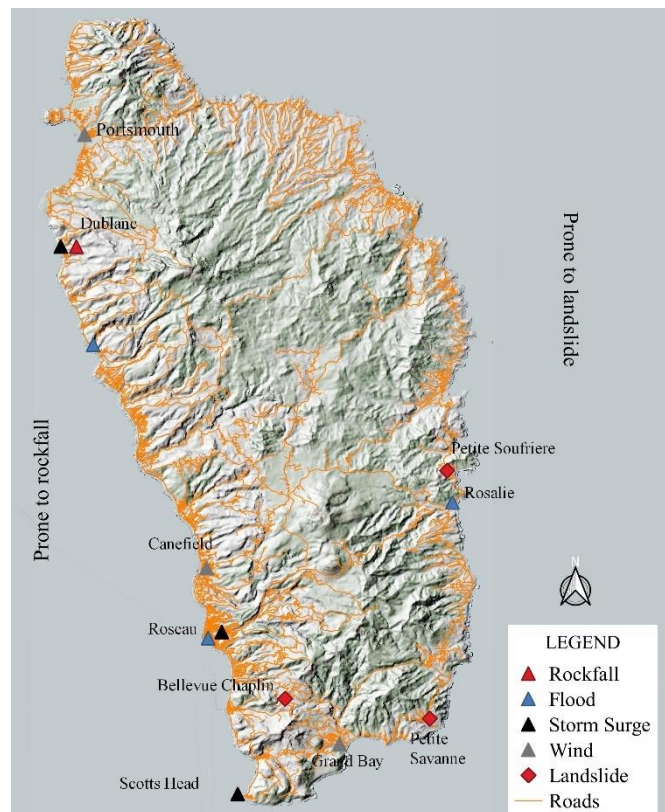
6.2.   Impact chain: Dominica

Figure 11 shows the impact chain of the whole island. It is divided into the main event which is TC Maria caused due to certain atmospheric factors. The primary hazards or the hazards that caused a chain of other hazards were high wind gusts and heavy precipitation. The predisposition factor of the terrain plays an important role in the formation of the cascading hazards (stated by government officials during field survey). Due to steep and rugged topography along with fractured and heavily disjointed rock fragments, with high wind gusts, these rock fragments gets pushed down under gravity and causes rockfall in western coasts. On the eastern coast, similar condition but due to gentler slope and different soil texture, rainfall mixes with the soil and causes huge landslides. Due to TC Maria, soil became overly saturated, leading to susceptibility of landslides. High wind gusts along the coastal regions caused storm surge. With heavy rainfall, the discharge of the rivers increased substantially causing inland flooding. Deposition of sediments brough down by landslides and rockfall along the coasts lead to change in coastal morphology and increase in sediment content of water affecting marine biology.
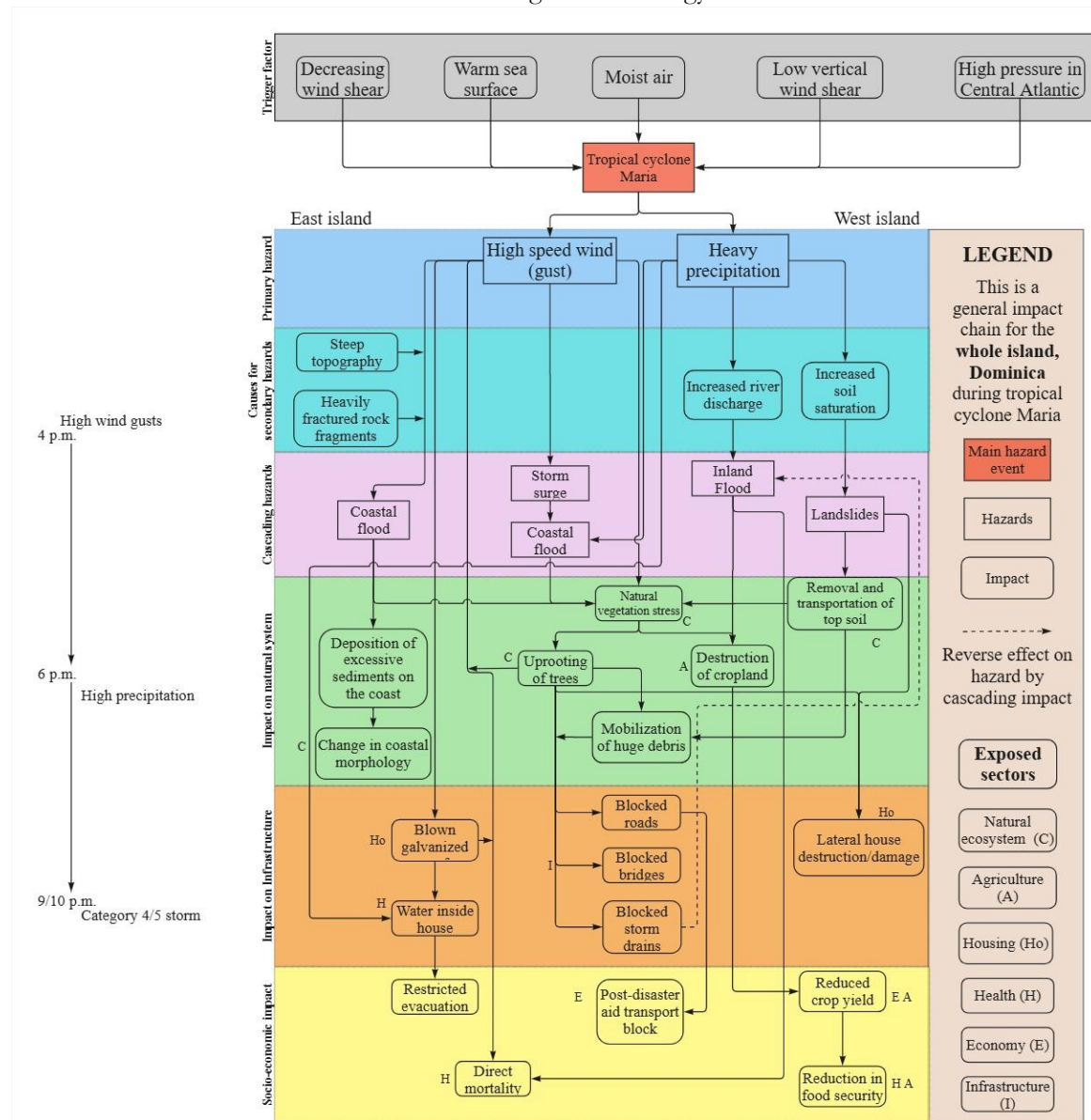

Figure 11: General impact chain for Dominica

Uprooting and throwing of trees by wind gusts or tree and soil mass movement by landslide is a direct impact on nature. Destruction of cropland also occurred throughout the island due to a combination of i) high wind gusts ii) flooding or iii) deposition of debris and sediments. The impact on infrastructure was also severe according to citizens. Landslide and rock fragments hitting or covering houses, bridges and roads are a direct threat to the community. The most prominent impact noticed was blockage of roads and bridges which hindered the evacuation during the event. Debris brought downstream blocked house entrances which also prevented inhabitants to go to shelters. Flood and debris entering ground floor were widespread. Wind hazards were also significant in various regions, including Portsmouth, Canefield in Roseau, and Grand Bay, among others. Trees and building roofs getting thrown and hitting other structures caused direct casualty to infrastructure. With roofs blown away, water entered the houses easily making it difficult to take shelter within the house. Blocked storm drains had a reverse impact on inland flooding. With water unable to escape into the sea due to the blockage, it flooded laterally increasing the severity of inland flooding.

Citizens estimated the timeline of hazards taking place, and the study reflects the conclusion that high wind gust started around 4 p.m. after which it took 2 hours to reach a peak precipitation. The storm reached category 5 at night. The information on initiation of TC Maria and reach its peak intensity was similar and thus validated by the report in DMS, (2017).

To focus on the hazard interactions specifically for the chosen case-study regions for this study, separate impact chains have been created. Figure 12 shows a separate impact chain for capital city of Roseau. The impact chain has similar hazard impacts however, not all hazards are present in this parish. From the interviews with CREAD, Red Cross and DRM of Dominica, information of storm surge and flooding bring the most prominent hazards observed in Roseau was collected. Substantial damage was caused to infrastructure by debris brought by rivers. Organizations like Sea and Air Authority (DASPA) had a strong impact from the cyclone event according to Dominica government officials. Canefield airport at Roseau was impacted by strong winds and debris materials from flood. Much of the debris was concentrated near Potterville which blocked roads and sewers. Woolridge Bay was impacted by coastal surges and flood. Water intrusion in the fisheries sectors caused loss of appliances and roof damage from winds stirred food insecurity which affected supporting sectors like market vendors. Blockage of power lines from debris and impact on electric poles by flood, nation-wide power outage occurred. Power outage caused complete hinderance to hospital machineries. With rainwater and debris entering buildings, Princess Margaret Hospital functional capacity reduced by 15% (PDNA, 2017). Apart from health, communication and infrastructure sectoral damage, cultural and tourism sector also faced impacts as well. Damage to hotels near the coast in Roseau affected the cruise industry (PDNA, 2017). During the interviews with the citizens, cyclone event, debris on roads hindered people (17 out of 20 people surveyed) to reach shelter zones since it was impossible to walk across piled up debris. Thus, they were stuck in their homes without proper cyclone shelter facilities causing evocation hindrance.

Figure 12: Impact chain for Roseau
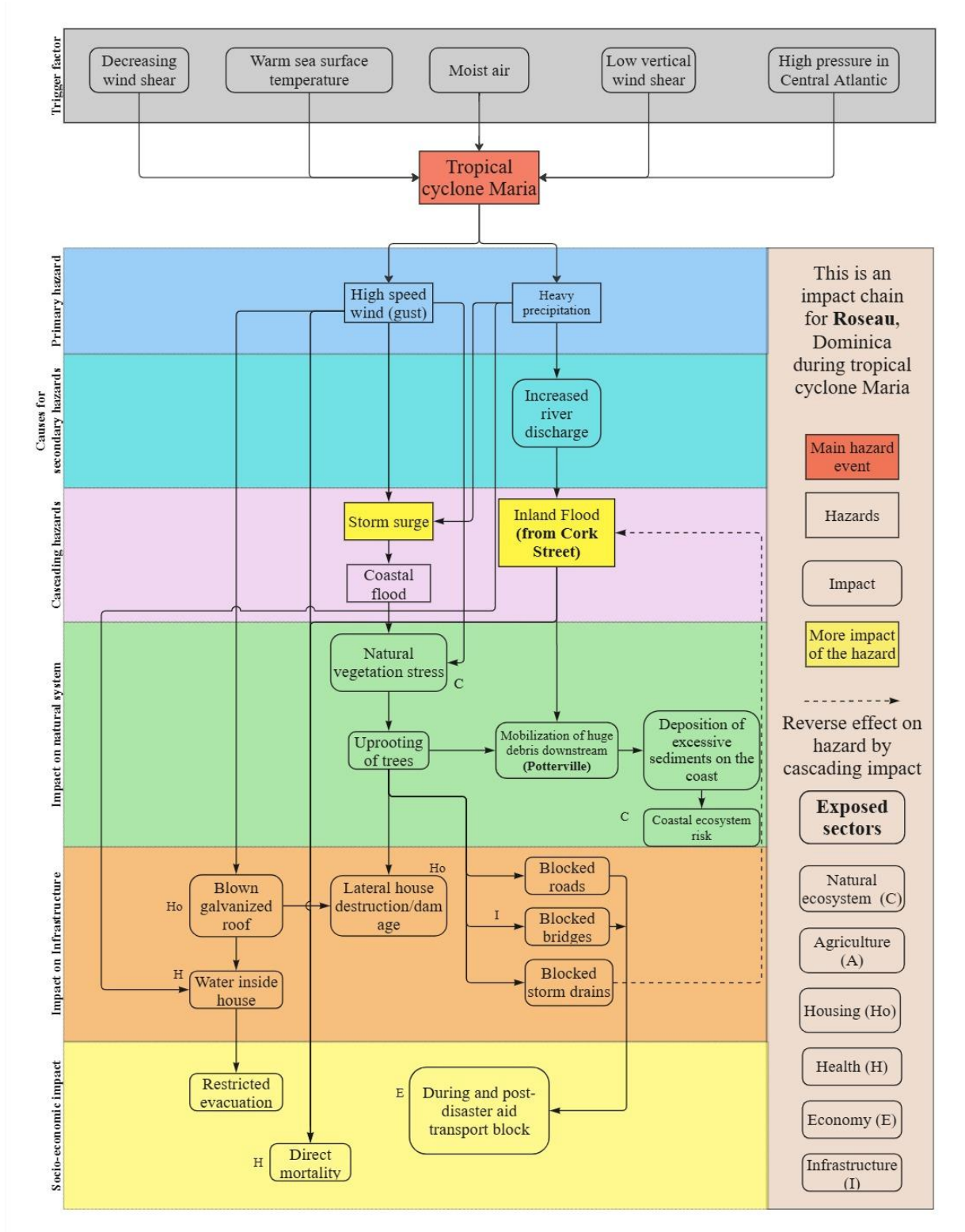
Figure 13 shows the impact chain for Portsmouth. According to citizen's survey, this regions witnessed more wind gusts and related damage compared to flood and landslides. The debris brought by the rivers or wind accumulated in this region, but the flooding happened in Picard, a downstream regions adjacent to Portsmouth, due to is lower altitude.
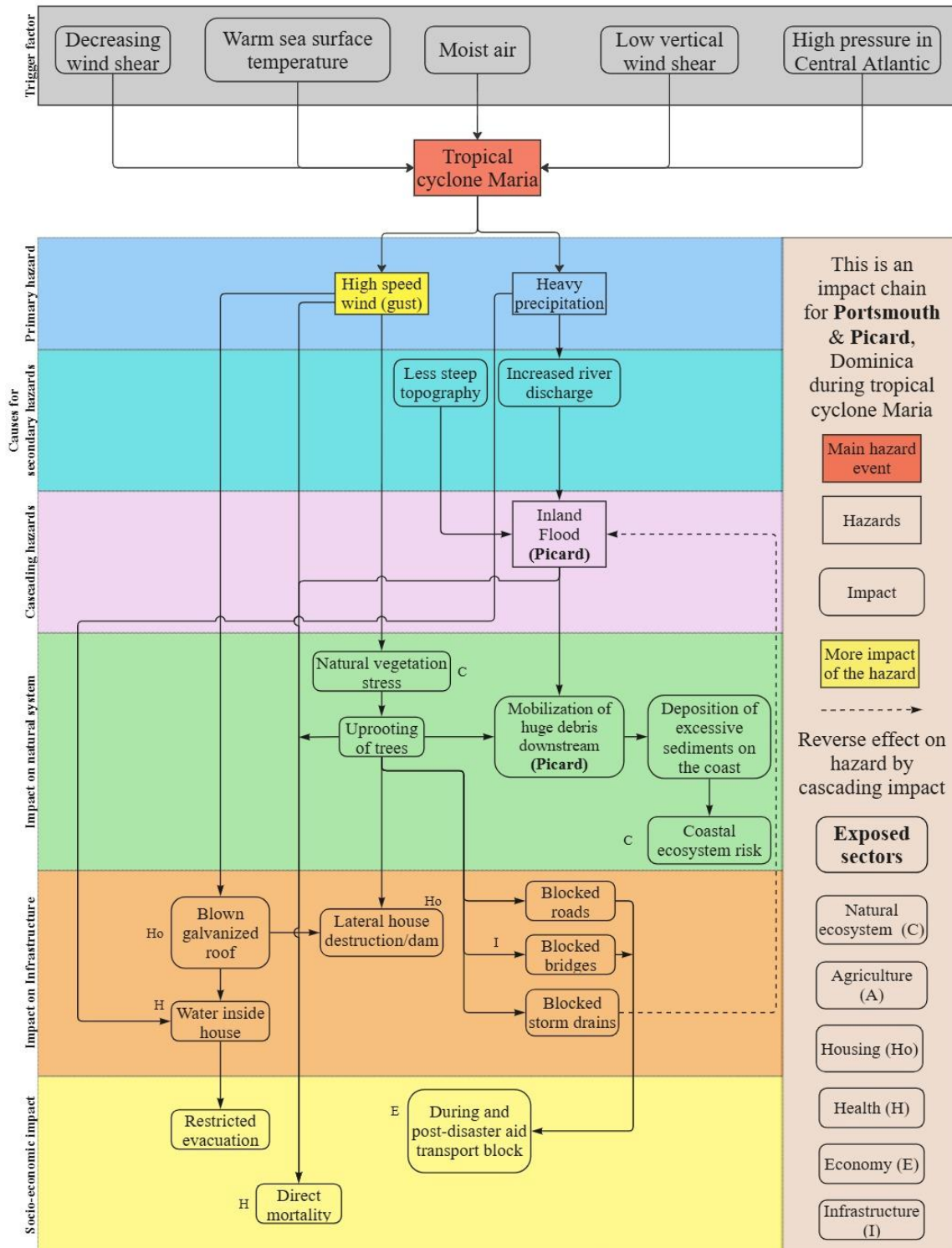

Figure 13: Impact chain for Portsmouth

According to inhabitants the region of Portsmouth was filled with debris after the storm, building materials and tree logs, however, around their neighborhood was completely dry, indicating the absence of severe flood situation. The presence of debris blocked many people reaching shelters in time, locking them in their houses without proper cyclone coping strategies. Damage of large cargo sheds, terminal buildings was reported to have major roof damage without much damage to the pier near the coast. Damage to these sheds mostly occur due to high wind gusts, and minor damage to pier can be due to less flood activity, unlike in Roseau (PDNA, 2017). According to TC Maria post damage assessment reports, complete rehabilitation took place for the ports worth US$3.56M. Cruise terminals and berths also underwent complete recuperation which incurred around US$4M. Apart from infrastructure, food sector also had a rough impact. Lack of electricity or loss or transmission lines caused disruption of perishable food storage like fishes that reduced the amount of food. Lack of electricity impacted the livelihood of the fishermen and market vendors in general.

Figure 14 shows the impact chain of Grand Bay, another case study region where the prominent hazards were different from Roseau and Portsmouth. The prominent hazards are highlighted in the impact chain, which shows that high wind gust was particularly devastating than any other hazard. The information was concluded after surveying 7-8 people in Grand Bay. Although this region has similar topography like Portsmouth, there were evidence of coastal flooding from field survey from the interviews conducted. Being a hilly region like Portsmouth, Grand Bay received heavy wind gusts. Having embankment near the coast, there were no high swells from the sea, however, floodwaters scoured banks which indirectly destabilized the buildings causing damage. The indirect impact of floodwater destroying banks and buildings were also presented by Battut et al., (2023). As indicated in the impact chain, deposition of heavy fluvial sediments caused coastal risks leading to shoreline movement.

The observed interactions between wind, landslide and flood processes during TC Maria can be interpreted from the impact chains. Water logging or flood situations were the most widespread and common throughout the whole island. Buildings and bridges were severely affected by landslide, wind and flood during TC Maria. In higher terrain regions like Portsmouth and Grand Bay, wind gusts were very strong blowing galvanised roofs, causing water to enter the buildings. High-rise buildings like Treasury building in Roseau had water inside he buildings from windows broken by wind gusts. Disruption of electric poles, shortage of electricity was caused due to landslides and wind gusts. Storm surges caused wreckage in the coastal areas like Roseau where houses were completely washed by strong waves. Debris from inland was also brought by landslide and flood waters, filling the coastal regions with excessive debris material. Natural vegetation was removed by landslides, destroyed by flood and uprooted by wind. Sewage pipes and storm drains being blocked caused inland flooding which might not have occurred as the same intensity had the water being able to pass through the drains. The storm drains also were not well equipped to accommodate the amount of debris-mixed water at once. Being out of capacity, some drains were severely damaged collapsing causing blockage by itself.

Combined impact of hazard was noticed prominently on the infrastructure. Besides blowing roofs and broken windows, flood water scoured under the houses and washed away the foundation leading to building collapse. In certain regions like Coulibistrie, houses near the coast were completely destroyed having debris remains and marks inside houses. Both blown roof, destroyed walls and debris marks were noticed (seen during field survey). Some bridges were also destroyed due to the impact of debris and water. Evacuation was hampered due to the impact of the hazards. Debris brought downstream by
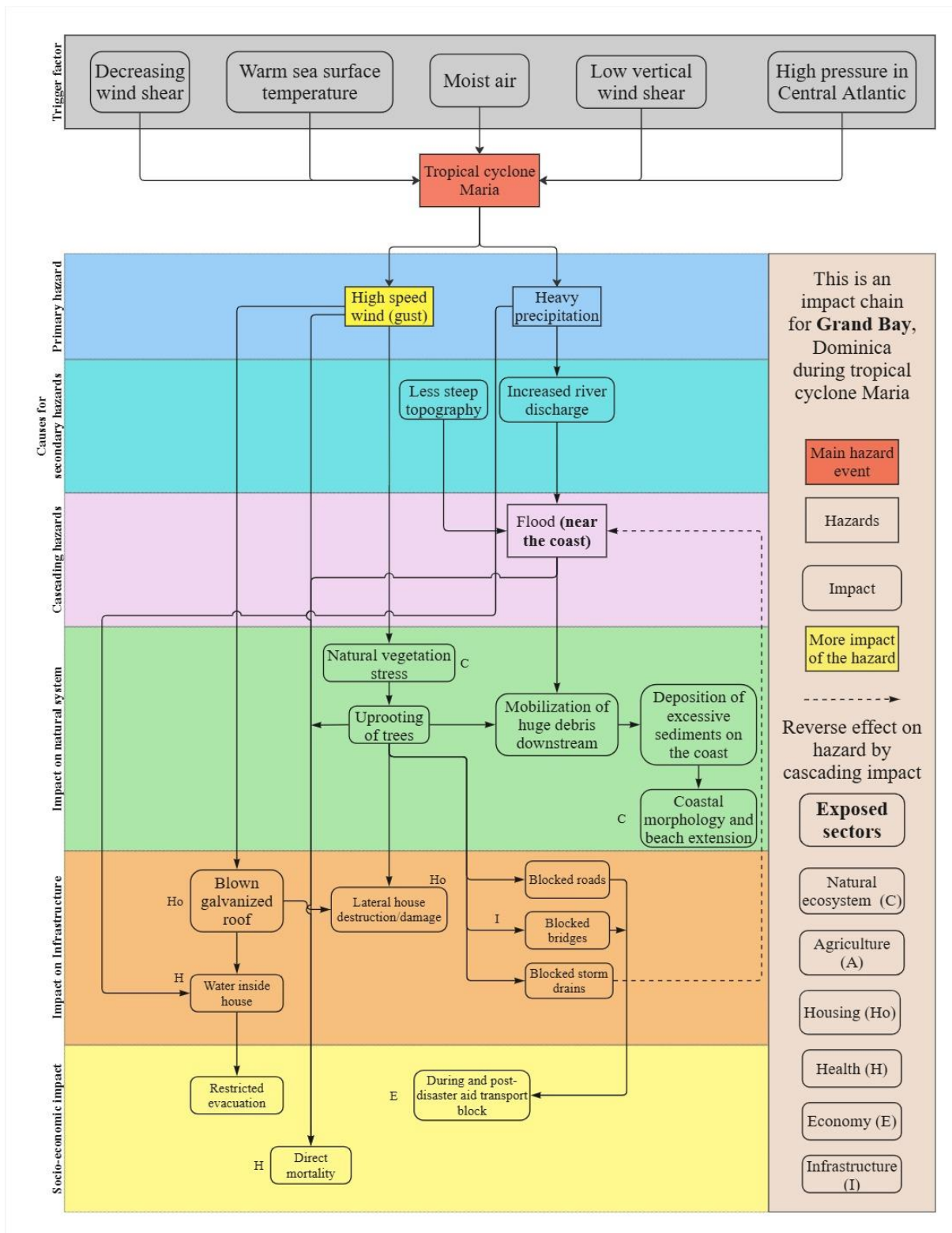
Figure 14: Impact chain of Grand Bay

landslide and flood blocked the house entrances and roads leading to evacuation centres. Wind gusts made it difficult for people to stay in their homes due to wreckage of roof and windows. Airports like Canefield and cruise berths in Roseau had an impact from both wind gusts and flood waters, among others.

6.3. Damage interpretation

Visual damage interpretation was done adhering to certain rules mentioned in section 5. An example is shown in Figure 15. It shows classification based on different types of hazard using bird's eye view of buildings.

Figure 15: Damage interpretation guide: Red box indicates wind impact since roof is covered with tarp, purple box shows less wind damage with less tarp cover; orange box highlights no roof damage and yellow box indicated combined destruction of hazards causing complete destruction

Figure 16: Damage interpretation, Portsmouth

Portsmouth has open spaces which increases the speed of wind unlike in Roseau, for which there uprooted tree regions more in Portsmouth. Houses stated 'intact' in Portsmouth have concrete ceiling which made it difficult for wind to blow the roofs away. See section 15 appendix for location of Figure 15 and Figure 17.

High and low wind impact was also visualized during the assessment. Figure 17 shows three different levels of wind impact mainly low which only some segment of the roof blown (light green circle). Second kind is high where interior is exposed meaning the entire roof is blown making interior vulnerable to precipitation and entrance of objects from outside during TC. The last kind is no impact (dark green circle). No impact can be due to effective galvanization of roof with the structure which citizen mentioned they did after TC Erika to secure their roofs from blown away.
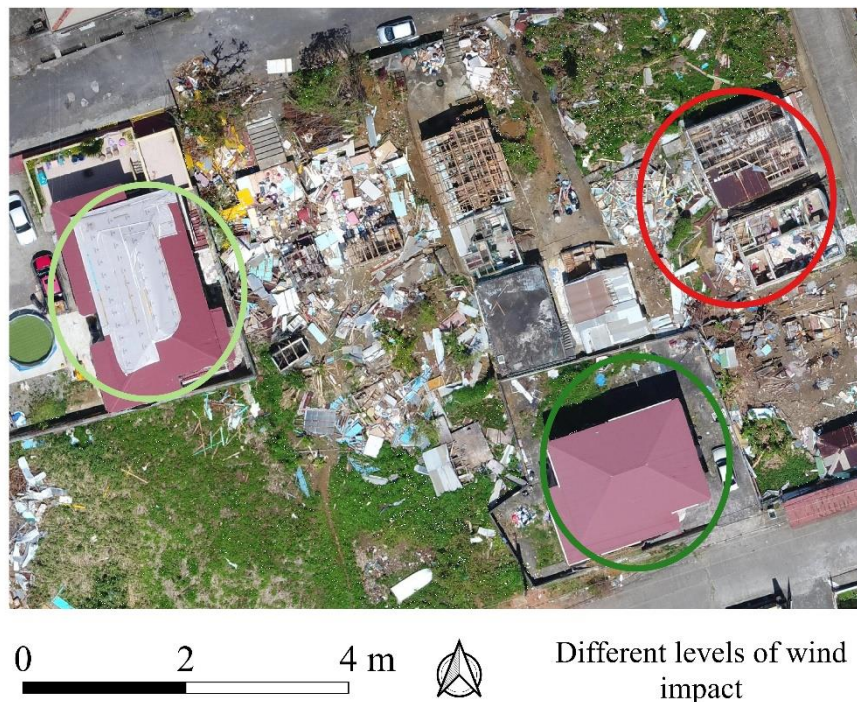
Figure 17: Different levels of wind impact: Light green: medium; dark green: less; red circle: high

6.4.   CityFFD: without topograhy, Roseau

Figure 18 shows the building footprint along with the domain or boundary box used for the simulation. The unit for paraview result are in meters.

In the wind speed calculated layer in Figure 19, the blue color depicts lower wind speed and as it moves to red, the wind speed gets higher (red being highest). The maximum wind speed shown here is 7.5 m/s. With minimum wind speed 0.04 m/s, results from CityFFD wind model (.vtk) are time-averaged for the period of weather data chosen to be simulated. The averaged wind is seen to enter from the northern boundary hence, northern region has the highest wind speed of i.e., at its entrance which gradually reduces to 0 m/s as it moves south.
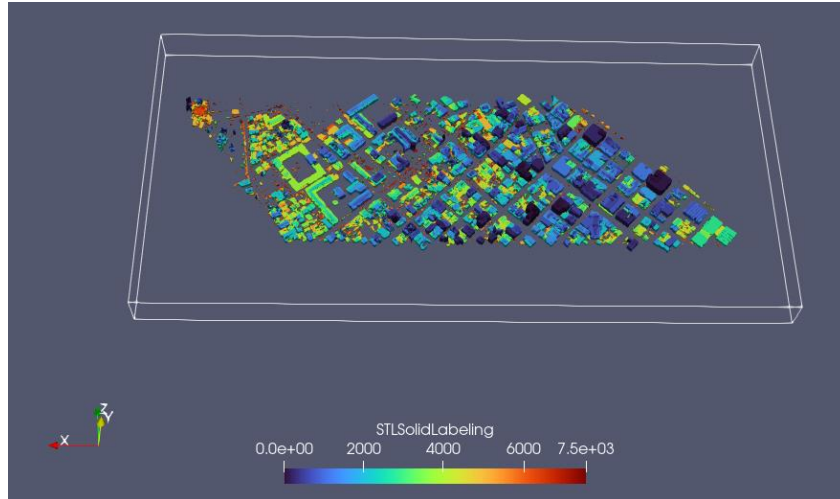
Figure 18: Building footprint and associated domain

Wind simulation shows relatively higher wind speed around the building footprint compared to the locations of the buildings. Wind speed is seen to be higher between the buildings and lower, on the immediate edges of the buildings. It shows the neighboring regions around buildings, where due to the blockage of wind from height of buildings, wind speed is less (Figure 19). However, on the streets speed slightly increases. This is reflected in reality, the wind speed is high in the areas between the buildings where wind can flow freely and have higher speed. Around the immediate edges of the buildings, wind speed decreases to 4m/s due to friction with building surface. The higher wind speeds observed between buildings and the corresponding decreases at the immediate edges can be theoretically explained through the lens of drag forces and the principles of fluid dynamics. The drag forces exerted by buildings on the passing wind result in slower speeds near the structures and faster speeds in the unobstructed spaces between them. Wind direction might have varied during TC event, so a multi-angle modeling might be also effective along with wind speed.
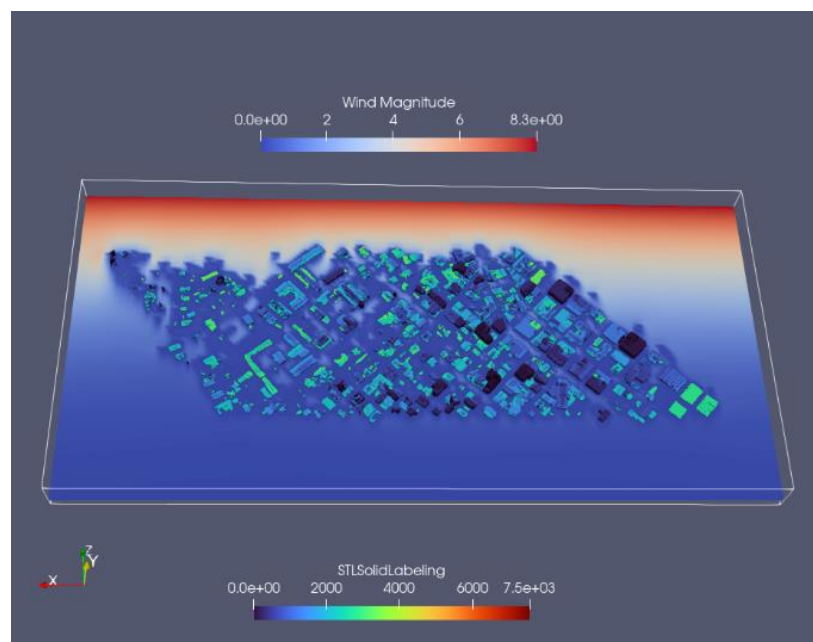
Figure 19: Wind speed calculation in paraview

Figure 20 shows the interpolated wind speed calculated in QGIS. As stated it was exported from paraview and interpolated in QGIS using IDW. The red region is associated with higher wind speed which gradually decreases as the wind moves south (dark blue). The interpolated map shows a straight red line at the northern side of the map with a slight imprint of the buildings layers that have lower (darker blue) wind speed. The maximum and minimum wind speed values (0.04 and 8.4m/s) calculated without y-axis (height factor) in QGIS are approximately same as that of paraview wind speed calculation with y-axis.

Wind speed (m/s)

0.04   8.479
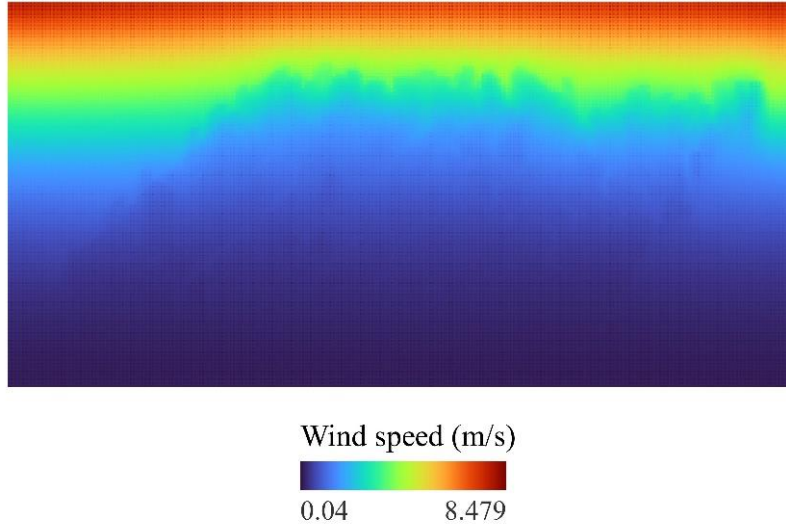
Figure 20: Wind speed interpolated in QGIS

The overlay of Figure 19 with building footprint was not successful due to variation in the format of both files. Figure 20 is point averaged data for u and v components of wind. Despite similar projections, the two layers do not seem to overlap efficiently (see section 14 appendix).

Validation using damage interpretation results

The damage interpretation map shown in Figure 21 corresponds to the same regions depicted in Figure 19. However, the orientation of the buildings between Figure 19 and Figure 21 does not align perfectly. Following the CityFFD simulation, the orientation of the buildings appears to have changed by nearly 180°. In Figure 21, the north arrow is oriented towards the southwest. The original map orientation was altered in QGIS to match the orientation of Figure 19. This alteration can influence the interpretation of the initial wind direction entering the model domain.

The wind simulation results do not accurately capture the physical behavior of the TC event. The model assumes that wind enters the boundary without obstruction, implying that wind will not be blocked by obstacles immediately outside the model domain (indicated by the red box in Figure 8). However, in reality, boundary conditions do not exist as there are buildings surrounding the model domain. Thus, the assumption of free wind flow used in the model is not applicable in this scenario. Furthermore, the damage interpretation map includes topographic effects that are not captured by CityFFD. Consequently, validating the model results against the damage interpretation map is not reliable.

Damage interpretation

■ Flood ■ Intact roofs ■ Storm surge and wind ■ Wind ■ Wind and flood

0   100   200 m

Figure 21: Damage interpretation, Roseau

6.5.   CityFFD: with topography, Roseau

Figure 22 shows the geometry file that was exported from QGIS along with the simulated .vtk file (white outline border). In the wind speed calculated layer in paraview, time-averaged wind speed is very uniform unlike the previous simulation as it does not show any variation with the effect of topography/structures. It does not capture deflection in wind with topography and has very clean transitions between windspeed values. Speed has increased in this simulation by approximately 13m/s for the same weather data file used in previous simulation without topography. The arrow flow through the buildings or structures without any interaction or deflection.
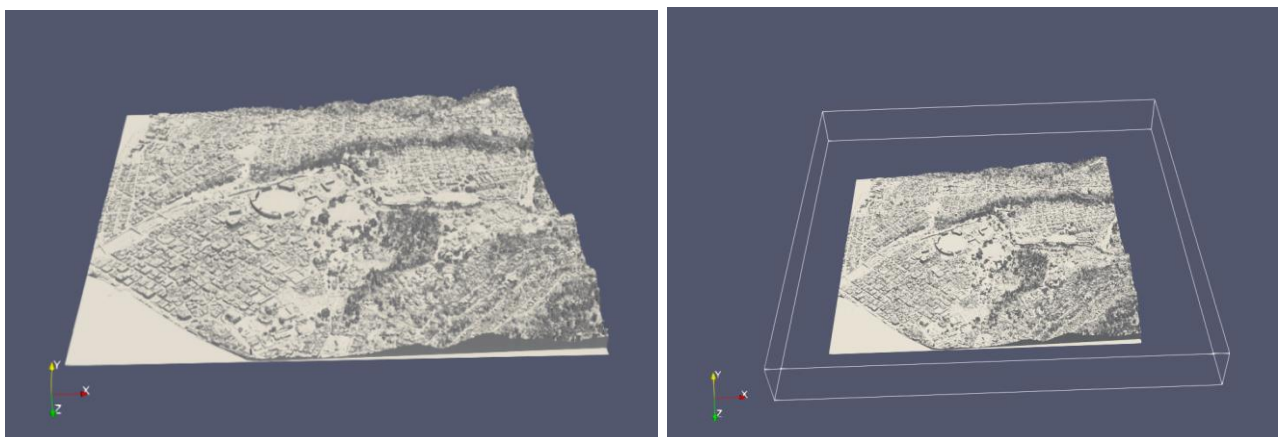
Figure 22: Left image shows the DSM used as .stl; Right image shows .stl with associated domain (outline)

Although the scale of CityFFD simulation including topography is effective to capture the details of tree impact, along with buildings and topography, .stl geometry file was not read by the model. Externally sourced geometry .stl file for instance, QGIS as used in this section, is not readable by the model which should be taken into account. The resolution should be at a building level to capture the multi-directions of wind when interacting with standing structures. Like CityFFD model, any other CFD model, based on solving the Navier-Stokes equations allowing prediction of fluid flow characteristics such as velocity, pressure and temperature distributions that can capture topography will be beneficial to deduce hazard interaction mentioned in the impact chains. However, boundary conditions should be simulated efficiently without the assumption of free-flow of wind outside the domain. To capture the physical behaviour of TC event, a larger area is required to be simulated. For a larger extent, computationally efficient model and user capacity is required. CtiyFFD is seen to be not effective in capturing wind patterns during TC event, due to boundary conditions and inability to simulate large areas lacking computation capacity.

7.   ETHICAL CONSIDERATIONS

The UNDP datasets were obtained by the Faculty of Geo-information Science and Earth Observation, University of Twente explicitly for research purposes. These datasets were used exclusively for the purpose of this research. These datasets are subject to specific usage constraints. The data was employed exclusively for the purposes outlined in this research and was not disseminated to external parties. Forensic field investigation was conducted by keeping the information generic. Information about specific home location, names of interviewees if required, were and will not be published. Also, the field investigation did not indulge in personal information of the people, but only corresponds to the hazard events interviewees witnessed during TC Maria. Storage of the collected data will be strictly encrypted and refrained from being made public without tracking any information back to original source. Consent was asked during the interviews to be recorded or for storage of data provided verbally.

8.   DISCUSIONS

Destruction by hazard interactions happened throughout the island with certain regions showed in Figure 10 having higher density of hazard interactions. Hence, for specific regions having most impact is difficult to specify for TC Maria. Summary of the interactions perceived during field survey reflects on RQs 1.

Table 5: Summary of interactions (single and combined hazard) during TC Maria observed/collected from citizens in field survey

Type of interaction	Perceived/recorded evidence
High wind gust increasing changes of rockfall	Bare mountain surfaces with rock outcrops
Wind gust and infrastructure impact buildings	Perceived evidence: Blown roofs
Landslide impact on vegetation/soil	Mountains predominantly covered with vegetation; however, certain patches without vegetation
Flood/ landslide and infrastructure impact buildings, storm drains	Abandoned houses exhibit broken walls and contain debris and floodmarks inside
Coastal flood impact on infrastructure	Citizens remarks on house destruction due to flood near coasts

Table 5 shows the types of hazard interactions along with evidences noticed or heard during field survey in Dominica.

The interaction of the hazards are well described in impact chains. Intricate inter-relationship between the hazards required high-resolution modelling which was portrayed by CityFFD. Resolution of CityFFD, capable of modelling areas less than 1 km with resolutions under 10 m. The high-resolution is evident in capturing multi-hazard interactions of high-resolution mentioned in impact chains. Comparing it with mesoscale wind models like WRF, these operate at larger scales (1-10 km domains, resolution over 100 m) (H. Li et al., 2021). However, they can be designed for various scale and resolution types (Skamarock & Klemp, 2008). The resolution for WRF models, might not be suitable for capturing intricate multi-hazard interactions at a building level. WRF can be coupled with microscale models for wind energy applications as shown in study by Dzebre et al., (2021), however, CityFFD are more specialised for high-resolution

turbulent flow simulations. Like CityFFD, Parallelized Large-Eddy Simulation Model (PALM) is a CFD model (Krutova et al., 2023) capable for offshore wind prediction. It uses incompressible Navier-Stokes equations in Boussinesq approximated form. PALM is considered capable of simulating in high-resolution within larger domains (Maronga et al., 2020) which was one of the drawbacks in CityFFD. Study by Nazarian et al., (2019), shows that PALM is versatile in capturing complex terrain, urban environments and can represent topography[2].

8.1.   Limitations

Methodology on the process of UNDP data was unavailable since it was received from a secondary source. Hence, the quality of this dataset is not verifiable. Also, the geo-location of building points for the various damage levels were not accurate, thus, the houses visited in the field might not have been in correspondence to the highest damage level as shown in map. With a short man-power and a duration of 6 -7 days, covering more houses would have been a challenge. Given the situation, 20 houses in total were covered for survey, with the condition we also had to fly drone and get images for other research purposes. The tenure of this field visit coincided with Dominica carnival festival 2024. For this reason, many people were outside their houses and we did not have people to interview with. Hence, the span of the field survey and the dates had affected number of houses surveyed and people interviewed. This reduced the number of houses with people inside to talk with since most of the houses were empty. However, the result obtained from the citizens' aligned with each other since the information was very similar. But there is always a doubt in the delivery of information from people about the experience during a massive TC event. Confusion and misinterpretation of the ongoing events can be very likely to occur as the citizens could neither see anything outside or go outside to inspect the hazard. All the information was either from what they heard, for instance, sound of high wind gusts or heavy pouring of rain and falling building roofs and tress nearby or what they witnessed at the end of the hazard- debris and piles of tree. Thus, their interpretation of the hazard events outside might be subjective and blurry.

During the post-disaster visual inspection utilizing drone imagery, it was observed that numerous structures had undergone provisional roofing measures, complicating the assessment of the actual extent of damage. Consequently, the accurate number of buildings affected may have been impeded. Initially, the outcomes of the visual inspection were intended to be corroborated through the integration of findings from wind modeling and other concurrent hazard assessments. However, discrepancies in the wind model predictions hindered the progression of this validation process.

Table 6 shows various tests run with different scales/resolution/topography before having a successful result. One of the main issues faced was lack of computational capacity during this study. All the combinations mentioned are capable of capturing wind interaction at a building level or at 0.5 m resolution if DEM/DSM is used.

Normally in weather models, depending on the resolution of wind data, downscaling of mesh grid file is performed. For instance, with 11 km resolution of wind components, models are initially simulated with 10 km resolution, then 5 km and then it gradually reduces, visualizing and interpreting the changes in results. However, for this study, the maximum length of the geometry (.stl) file is 1700 m. Overlaying a 10 or 5 km grid mesh file on top, will not be logical since one cell of the grid will be larger covering the study

---

[2] https://palm.muk.uni-hannover.de/trac/wiki/doc/tec/topography

area and result in a uniform wind speed layer. Thus, for this study such strategic downscaling was not performed and a grid size of 5 m was selected to capture structure details within each cell.

Table 6: Attempts made for wind simulation integrating various plugins and external software

Resolution	Plugin	Layers	Extent	Status
0.5 m	Qgis2threejs: designed to visualize DEM and vector data in 3D	Topography	Red box shown in figure 8	Computational overload/ problem in export
Vector file with 3D building	Qgis2threejs	Buildings with relative height of terrain	Red box shown in figure 8	Computational overload/ problem in export
0.5 m	DEMto3D	Topography	Red box shown in figure 8	Error in combining building .stl in blender
0.5 m	Qgis2threejs	Topography overlayed with building	Same as red building footprint in figure 8	Computational overload/ problem in export
0.5 m	DEMto3D	DSM	Red box shown in figure 8	Success

8.2.   Future implications

This work have laid the initial concept for refining wind speed around cyclone-prone regions like Dominica. Models like WRF predict and analyze the wind speed throughout the country. However, specific wind gust related damage to buildings at a very high resolution is important to understand the multi-hazard interaction. This work have laid the initial concept for refining wind speed around cyclone-prone regions like Dominica. Models like WRF predict and analyze the wind speed throughout the country. However, specific wind gust related damage to buildings at a very high resolution is important to understand the multi-hazard interaction. With the wind simulation improvement, many research ideas can be taken for future researchers. One of being, overlaying the wind speed layer with landslide and flood hazard layer to oversee which regions have what specific hazard combination. This can give a glimpse of understanding the concentration of one particular hazard in one region and absences of the same hazard in another. For instance, in Roseau flood hazard might have been more widespread than high wind speed; or Portsmouth would have shown higher wind speed and less flooded regions. The purpose of this research would give first-responders to distribute resources according to the dominance of hazards in targeted regions. Flood regions will get more medicines of cholera and life jackets or helicopter services whereas, high wind gusts regions would get materials to build roofs and temporary roof covers. Physical Planning authorities can also have building codes according to the relevance of hazards. Flood-prone of landslide regions should have high built houses, building materials can be made short-term water resistant. Roofs can be structured to be more strong and permanent for withstanding wind gusts. For multi-hazard

interaction assessment, it is essential to have flood and landslide hazard map as the same resolution as wind simulation result. Difference in resolution can cause underestimation of hazard interactions taking place.

Another branch of research could be to analyse how the vulnerability curve towards wind changes once a building is hit by flood. The change in fragility curve with hazard gradually can hold a significant foundation in assessment of damage during cascading hazards like earthquake, cyclone, etc. Long-term planning for building structures can be performed by the government by building multi-hazard resistant buildings. Also, when one hazard subsides, referring to the changes in vulnerability curves, steps can be taken to reduce collapse risk from a future hazard event. For another dimension of research without considering the multi-hazard interaction, results of wind speed can be combined with building material information from UNDP dataset. The process will provide vulnerable houses according to the type of materials in various wind speed zones.

Computational capacity of the users laptop is also a matter of concern since not only wind model takes time, without GPU, serious harm can be done to the laptop if run solely on CPU. A proper GPU connection or internal GPU environment from user's organisations should be used.

9.   REFERENCES

Achu, A. L., Aju, C. D., Di Napoli, M., Prakash, P., Gopinath, G., Shaji, E., & Chandra, V. (2023). Machine-learning based landslide susceptibility modelling with emphasis on uncertainty analysis. *Geoscience Frontiers*, *14*(6), 101657. https://doi.org/10.1016/J.GSF.2023.101657

Adcock, C., Henry De Frahan, M., Melvin, J., Vijayakumar, G., Ananthan, S., Iaccarino, G., Moser, R., & Sprague, M. (2022). *Hybrid RANS-LES of the Atmospheric Boundary Layer for Wind Farm Simulations: Preprint*. https://doi.org/10.2514/6.2022-1922

Alimohammadi, M., & Malakooti, H. (2018). Sensitivity of simulated cyclone Gonu intensity and track to variety of parameterizations: Advanced hurricane WRF model application. *Journal of Earth System Science*, *127*(3), 1–15. https://doi.org/10.1007/S12040-018-0941-4/TABLES/3

Apa) Mehravar, S., Razavi-Termeh, S. V, Moghimi, A. ;, Ranjgar, B. ;, Foroughnia, F. ;, & Amani, M. (2023). Flood susceptibility mapping using multi-temporal SAR imagery and novel integration of nature-inspired algorithms into support vector regression Flood susceptibility mapping using multi-temporal SAR imagery and novel integration of nature-inspired algorithms into support vector regression Flood susceptibility mapping using multi-temporal SAR imagery and novel integration of nature-inspired algorithms into support vector regression. *Journal of Hydrology Citation*, *617*, 129100. https://doi.org/10.1016/j.jhydrol.2023.129100

Arthur, W. C. (2021). A statistical-parametric model of tropical cyclones for hazard assessment. *Natural Hazards and Earth System Sciences*, *21*(3), 893–916. https://doi.org/10.5194/NHESS-21-893-2021

Atun, F. (2023). *Forensic Analysis of historical disasters to develop quantifiable multi-hazard impact chains models*.

Barclay, J., Wilkinson, E., White, C. S., Shelton, C., Forster, J., Few, R., Lorenzoni, I., Woolhouse, G., Jowitt, C., Stone, H., & Honychurch, L. (2019). Historical Trajectories of Disaster Risk in Dominica. *International Journal of Disaster Risk Science*, *10*(2), 149–165. https://doi.org/10.1007/S13753-019-0215-Z

Barrantes, G. (2018). Multi-hazard model for developing countries. *Natural Hazards*, *92*(2), 1081–1095. https://doi.org/10.1007/S11069-018-3239-6/FIGURES/5

Battut, S., Rey, T., Cécé, R., Bernard, D., & Krien, Y. (2023). Responses and adjustments of the coastal systems of Dominica (Lesser Antilles) when faced with an extreme event: Hurricane Maria (September 2017). *Natural Hazards*, *116*(1), 151–191. https://doi.org/10.1007/S11069-022-05668-2/FIGURES/17

BBC. (2017). *Dominica profile - Timeline - BBC News*. https://www.bbc.com/news/world-latin-america-19409492

BenMoshe, N., Fattal, E., Leitl, B., & Arav, Y. (2023). Using Machine Learning to Predict Wind Flow in Urban Areas. *Atmosphere 2023, Vol. 14, Page 990*, *14*(6), 990. https://doi.org/10.3390/ATMOS14060990

Bernard, J., Lindberg, F., & Oswald, S. (2023). URock 2023a: an open-source GIS-based wind model for complex urban settings. *Geoscientific Model Development*, *16*(20), 5703–5727. https://doi.org/10.5194/GMD-16-5703-2023

Bevacqua, E., Suarez-Gutierrez, L., Jézéquel, A., Lehner, F., Vrac, M., Yiou, P., & Zscheischler, J. (2023). Advancing research on compound weather and climate events via large ensemble model simulations. *Nature Communications 2023 14:1*, *14*(1), 1–16. https://doi.org/10.1038/s41467-023-37847-5

Bodoque, J. M., Guardiola-Albert, C., Aroca-Jiménez, E., Eguibar, M. Á., & Martínez-Chenoll, M. L. (2016). Flood Damage Analysis: First Floor Elevation Uncertainty Resulting from LiDAR-Derived Digital Surface Models. *Remote Sensing 2016, Vol. 8, Page 604*, *8*(7), 604. https://doi.org/10.3390/RS8070604

Bonshoms, M., Ubeda, J., Liguori, G., Körner, P., Navarro, Á., & Cruz, R. (2022). Validation of ERA5-Land temperature and relative humidity on four Peruvian glaciers using on-glacier observations. *Journal of Mountain Science*, *19*(7), 1849–1873. https://doi.org/10.1007/S11629-022-7388-4/METRICS

Boudreault, L.-E. (2015). *Reynolds-averaged Navier-Stokes and Large-Eddy Simulation Over and Inside Inhomogeneous Forests*.

Brencich, A. (2010). Deep trench, landslide and effects on the foundations of a residential building: A case study. *Engineering Structures*, *32*(7), 1821–1829. https://doi.org/10.1016/J.ENGSTRUCT.2010.02.019

Browne, A. S. (2020). *FINAL EVALUATION OF HURRICANE MARIA OPERATION, DOMINICA RESPONSE TO RECOVERY*.

Bruneau, N., Loridan, T., Hannah, N., Dubossarsky, E., Joffrain, M., & Knaff, J. (2024). Modeling Variability in Tropical Cyclone Maximum Wind Location and Intensity Using InCyc: A Global Database of High-Resolution Tropical Cyclone Simulations. *Monthly Weather Review*, *152*(1), 319–343. https://doi.org/10.1175/MWR-D-22-0317.1

Bruyère, C. L., Done, J. M., Jaye, A. B., Holland, G. J., Buckley, B., Henderson, D. J., Leplastrier, M., & Chan, P. (2019). Physically-based landfalling tropical cyclone scenarios in support of risk assessment. *Weather and Climate Extremes*, *26*, 100229. https://doi.org/10.1016/J.WACE.2019.100229

Bryce, E., Lombardo, L., van Westen, C., Tanyas, H., & Castro-Camilo, D. (2022). Unified landslide hazard assessment using hurdle models: a case study in the Island of Dominica. *Stochastic Environmental Research and Risk Assessment*, *36*(8), 2071–2084. https://doi.org/10.1007/S00477-022-02239-6/TABLES/3

Carvalho, D., Rocha, A., Gómez-Gesteira, M., & Santos, C. (2012). A sensitivity study of the WRF model in wind simulation for an area of high wind energy. *Environmental Modelling & Software*, *33*, 23–34. https://doi.org/10.1016/J.ENVSOFT.2012.01.019

Chang, D., Amin, S., & Meteorology, K. E. (2020). Modeling and parameter estimation of hurricane wind fields with asymmetry. *Journals.Ametsoc.OrgD Chang, S Amin, K EmanuelJournal of Applied Meteorology and Climatology, 2020•journals.Ametsoc.Org*. https://journals.ametsoc.org/view/journals/apme/59/4/jamc-d-19-0126.1.xml?tab_body=pdf

Chen, R., Zhang, W., & Wang, X. (2020). Machine Learning in Tropical Cyclone Forecast Modeling: A Review. *Atmosphere 2020, Vol. 11, Page 676*, *11*(7), 676. https://doi.org/10.3390/ATMOS11070676

Czajkowski, J., & Done, J. (2014). As the Wind Blows? Understanding Hurricane Damages at the Local Level through a Case Study Analysis. *Weather, Climate, and Society*, *6*(2), 202–217. https://doi.org/10.1175/WCAS-D-13-00024.1

De Angeli, S., Malamud, B. D., Rossi, L., Taylor, F. E., Trasforini, E., & Rudari, R. (2022). A multi-hazard framework for spatial-temporal impact analysis. *International Journal of Disaster Risk Reduction*, *73*, 102829. https://doi.org/10.1016/J.IJDRR.2022.102829

Deltares. (2023). *Delft3D 3D/2D modelling suite for integral water solutions*.

DMS. (2017). *Hurricane Maria: Hydro-Meteorological Impact on Dominica*.

Do, C., & Kuleshov, Y. (2023). Multi-Hazard Tropical Cyclone Risk Assessment for Australia. *Remote Sensing 2023, Vol. 15, Page 795*, *15*(3), 795. https://doi.org/10.3390/RS15030795

Dorst, S. (2021). *Dominica Develops Resilience*. IMF. https://www.imf.org/en/News/Articles/2021/10/27/na110221-dominica-develops-resilience

Drakes, O., & Tate, E. (2022). Social vulnerability in a multi-hazard context: a systematic review. *Environmental Research Letters*, *17*(3), 033001. https://doi.org/10.1088/1748-9326/AC5140

Dzebre, D. E. K., Ampofo, J., & Adaramola, M. S. (2021). An assessment of high-resolution wind speeds downscaled with the Weather Research and Forecasting Model for coastal areas in Ghana. *Heliyon*, *7*(8), e07768. https://doi.org/10.1016/J.HELIYON.2021.E07768

Ebenhoch, R. (2015). *Simplified modeling of wind-farm flows*.

Ell, S. :, & Sprin, S. (1992). *NOAA Technical Report NWS 48 UNITED STATES DEPARTMENT OF COMMERCE National Oceanic and National eather Service Atmospheric Administration Sea, Lake, and Over aýd SULirges froý11 Hrrianes*.

Fobert, M.-A., Singhroy, V., & Spray, J. G. (2021). *InSAR Monitoring of Landslide Activity in Dominica*. https://doi.org/10.3390/rs13040815

Gao, Y., Wang, H., Liu, G. M., Sun, X. Y., Fei, X. Y., Wang, P. T., Lv, T. T., Xue, Z. S., & He, Y. W. (2014). Risk assessment of tropical storm surges for coastal regions of China. *Journal of Geophysical Research: Atmospheres*, *119*(9), 5364–5374. https://doi.org/10.1002/2013JD021268

Gardiner, B. A., Chen, Y. Y., Ruel, J. C., & Kamimura, K. (2022). Editorial: Living with tropical storms in a changing climate. *Frontiers in Forests and Global Change*, *5*, 988875. https://doi.org/10.3389/FFGC.2022.988875/BIBTEX

Ghosh, S. (2010). *POST-DISASTER BUILDING DAMAGE ASSESSMENT USING SATELLITE AND AERIAL IMAGERY INTERPRETATION, FIELD VERIFICATION AND MODELING TECHNIQUES 2010 HAITI EARTHQUAKE Final Report*.

Gill, J. C., & Malamud, B. D. (2014). Reviewing and visualizing the interactions of natural hazards. *Reviews of Geophysics*, *52*(4), 680–722. https://doi.org/10.1002/2013RG000445

Gill, J. C., & Malamud, B. D. (2016a). Hazard interactions and interaction networks (cascades) within multi-hazard methodologies. *Earth Syst. Dynam*, *7*, 659–679. https://doi.org/10.5194/esd-7-659-2016

Gill, J. C., & Malamud, B. D. (2016b). Hazard interactions and interaction networks (cascades) within multi-hazard methodologies. *Earth Syst. Dynam*, *7*, 659–679. https://doi.org/10.5194/esd-7-659-2016

Goldenberg, S. B., & Shapiro, L. J. (1996). Physical Mechanisms for the Association of El Niño and West African Rainfall with Atlantic Major Hurricane Activity. *Journal of Climate*, *9*(6), 1169–1187. https://doi.org/https://doi.org/10.1175/1520-0442(1996)009<1169:PMFTAO>2.0.CO;2

Government of the Commonwealth of Dominica. (2016). *Draft Dominica National Physical Development Plan*.

Goyes-Peñafiel, P., & Hernandez-Rojas, A. (2021). Landslide susceptibility index based on the integration of logistic regression and weights of evidence: A case study in Popayan, Colombia. *Engineering Geology*, *280*, 105958. https://doi.org/10.1016/J.ENGGEO.2020.105958

Gravley, D. (2001). *Risk, Hazard, and Disaster*.

Hadi Jafari, P., Gunnar, J., Hellström, I., & Gebart, B. R. (2017). *Turbulence Modelling of a Single-Phase Flow Cyclone Gasifier. 9*, 779–799. https://doi.org/10.4236/eng.2017.99047

Han, X., Chang, C., Guo, Z., Yin, S., Li, J., Li, H., Wang, R., & Li, Q. (2023). Comparison of deterministic wind speed generation models for wind erosion modeling. *Agricultural and Forest Meteorology*, *334*, 109438. https://doi.org/10.1016/J.AGRFORMET.2023.109438

Hersbach, H., Bell, B., Berrisford, P., Hirahara, S., Horányi, A., Muñoz-Sabater, J., Nicolas, J., Peubey, C., Radu, R., Schepers, D., Simmons, A., Soci, C., Abdalla, S., Abellan, X., Balsamo, G., Bechtold, P., Biavati, G., Bidlot, J., Bonavita, M., … Thépaut, J. N. (2020). The ERA5 global reanalysis. *Quarterly Journal of the Royal Meteorological Society*, *146*(730), 1999–2049. https://doi.org/10.1002/QJ.3803

Hochrainer-Stigler, S., Trogrlić Šakić, R., Reiter, K., Ward, P. J., de Ruiter, M. C., Duncan, M. J., Torresan, S., Ciurean, R., Mysiak, J., Stuparu, D., & Gottardo, S. (2023). Toward a framework for systemic multi-hazard and multi-risk assessment and management. *IScience*, *26*(5). https://doi.org/10.1016/J.ISCI.2023.106736

Howe, T. M., Lindsay, J. M., Shane, P., Schmitt, A. K., & Stockli, D. F. (2014). Re-evaluation of the Roseau Tuff eruptive sequence and other ignimbrites in Dominica, Lesser Antilles. *Journal of Quaternary Science*, *29*(6), 531–546. https://doi.org/10.1002/JQS.2723

Hu, L., Wen, T., Shao, Y., Wang, Q., Fang, W., Yang, J., Liu, M., Wang, X., Zhang, H., Bi, J., & Ma, Z. (2023). Economic Impacts of Tropical Cyclone-Induced Multiple Hazards in China. *Earth's Future*, *11*(9). https://doi.org/10.1029/2023EF003622

Hu, Q., Zhou, Y., Wang, S., & Wang, F. (2020). Machine learning and fractal theory models for landslide susceptibility mapping: Case study from the Jinsha River Basin. *Geomorphology*, *351*, 106975. https://doi.org/10.1016/J.GEOMORPH.2019.106975

Hu, T., & Smith, R. B. (2018). The Impact of Hurricane Maria on the Vegetation of Dominica and Puerto Rico Using Multispectral Remote Sensing. *Remote Sensing 2018, Vol. 10, Page 827*, *10*(6), 827. https://doi.org/10.3390/RS10060827

IPCC. (2023). Weather and Climate Extreme Events in a Changing Climate. *Climate Change 2021 – The Physical Science Basis*, 1513–1766. https://doi.org/10.1017/9781009157896.013

Islam, A. R. M. T., Talukdar, S., Mahato, S., Kundu, S., Eibek, K. U., Pham, Q. B., Kuriqi, A., & Linh, N. T. T. (2021). Flood susceptibility modelling using advanced ensemble machine learning models. *Geoscience Frontiers*, *12*(3), 101075. https://doi.org/10.1016/j.gsf.2020.09.006

Jury, M. R., Chiao, S., & Cécé, R. (2019). The Intensification of Hurricane Maria 2017 in the Antilles. *Atmosphere 2019, Vol. 10, Page 590*, *10*(10), 590. https://doi.org/10.3390/ATMOS10100590

Kappes, M. S., Keiler, M., von Elverfeldt, K., & Glade, T. (2012). Challenges of analyzing multi-hazard risk: A review. *Natural Hazards*, *64*(2), 1925–1958. https://doi.org/10.1007/S11069-012-0294-2/FIGURES/9

Katal, A., Mortezazadeh, M., & Wang, L. (Leon). (2019). Modeling building resilience against extreme weather by integrated CityFFD and CityBEM simulations. *Applied Energy*, *250*, 1402–1417. https://doi.org/10.1016/J.APENERGY.2019.04.192

Krutova, M., Bakhoday-Paskyabi, M., Reuder, J., Gunnar Nielsen, F., & Krutova mariakrutova, M. (2023). Self-nested large-eddy simulations in PALM model system v21.10 for offshore wind prediction under different atmospheric stability conditions. *Geosci. Model Dev*, *16*, 3553–3564. https://doi.org/10.5194/gmd-16-3553-2023

Lawrence, M. G. (2005). The Relationship between Relative Humidity and the Dewpoint Temperature in Moist Air: A Simple Conversion and Applications. *Bulletin of the American Meteorological Society*, *86*(2), 225–234. https://doi.org/10.1175/BAMS-86-2-225

Lee, K. H., & Rosowsky, D. V. (2005). Fragility assessment for roof sheathing failure in high wind regions. *Engineering Structures*, *27*(6), 857–868. https://doi.org/10.1016/J.ENGSTRUCT.2004.12.017

Li, H., Claremar, B., Wu, L., Hallgren, C., Körnich, H., Ivanell, S., & Sahlée, E. (2021). A sensitivity study of the WRF model in offshore wind modeling over the Baltic Sea. *Geoscience Frontiers*, *12*(6), 101229. https://doi.org/10.1016/J.GSF.2021.101229

Li, S., Sun, X., Zhang, S., Zhao, S., & Zhang, R. (2019). A Study on Microscale Wind Simulations with a Coupled WRF–CFD Model in the Chongli Mountain Region of Hebei Province, China. *Atmosphere 2019, Vol. 10, Page 731*, *10*(12), 731. https://doi.org/10.3390/ATMOS10120731

Li, Y., Huang, X., Li, Y. G., Chen, F. Bin, & Li, Q. S. (2022). Machine learning based algorithms for wind pressure prediction of high-rise buildings. *Advances in Structural Engineering*, *25*(10), 2222–2233. https://doi.org/10.1177/13694332221092671/ASSET/IMAGES/LARGE/10.1177_136943322210 92671-FIG18.JPEG

Li, Y., Shen, P., Yan, Y., & Zhou, W. H. (2022). Flood risk assessment of artificial islands under compound rain-tide-wind effects during tropical cyclones. *Journal of Hydrology*, *615*, 128736. https://doi.org/10.1016/J.JHYDROL.2022.128736

Lindsay, J. M., Stasiuk, M. V., & Shepherd, J. B. (2003). Geological history and potential hazards of the late-Pleistocene to Recent Plat Pays volcanic complex, Dominica, Lesser Antilles. *Bulletin of Volcanology*, *65*(2–3), 201–220. https://doi.org/10.1007/S00445-002-0253-Y/METRICS

Liu, B., Siu, Y. L., & Mitchell, G. (2016a). Hazard interaction analysis for multi-hazard risk assessment: A systematic classification based on hazard-forming environment. *Natural Hazards and Earth System Sciences*, *16*(2), 629–642. https://doi.org/10.5194/NHESS-16-629-2016

Liu, B., Siu, Y. L., & Mitchell, G. (2016b). Hazard interaction analysis for multi-hazard risk assessment: A systematic classification based on hazard-forming environment. *Natural Hazards and Earth System Sciences*, *16*(2), 629–642. https://doi.org/10.5194/NHESS-16-629-2016

Liu, C., Liao, X., Qiu, J., -, al, Hu, W., Scholz, Y., Yeligeti, M., von Bremen, L., & Deng, Y. (2023). Downscaling ERA5 wind speed data: a machine learning approach considering topographic influences. *Environmental Research Letters*, *18*(9), 094007. https://doi.org/10.1088/1748-9326/ACEB0A

Lozano, J. M., & Tien, I. (2023). Data collection tools for post-disaster damage assessment of building and lifeline infrastructure systems. *International Journal of Disaster Risk Reduction*, *94*, 103819. https://doi.org/10.1016/J.IJDRR.2023.103819

Luino, F., Cirio, C. G., Biddoccu, M., Agangi, A., Giulietto, W., Godone, F., & Nigrelli, G. (2009). Application of a model to the evaluation of flood damage. *GeoInformatica*, *13*(3), 339–353. https://doi.org/10.1007/S10707-008-0070-3/FIGURES/7

Manchia, C. M., & Mulligan, R. P. (2022). Hurricane wind-driven surface waves on a narrow continental shelf and exposed coast. *Continental Shelf Research*, *237*, 104681. https://doi.org/10.1016/J.CSR.2022.104681

Mandal, P., Maiti, A., Paul, S., Bhattacharya, S., & Paul, S. (2022). Mapping the multi-hazards risk index for coastal block of Sundarban, India using AHP and machine learning algorithms. *Tropical Cyclone Research and Review*, *11*(4), 225–243. https://doi.org/10.1016/J.TCRR.2023.03.001

Manikanta, N. D., Joseph, S., & Naidu, C. V. (2023). Recent global increase in multiple rapid intensification of tropical cyclones. *Scientific Reports 2023 13:1*, *13*(1), 1–12. https://doi.org/10.1038/s41598-023-43290-9

Maronga, B., Banzhaf, S., Burmeister, C., Esch, T., Forkel, R., Fröhlich, D., Fuka, V., Gehrke, K. F., Geletič, J., Giersch, S., Gronemeier, T., Groß, G., Heldens, W., Hellsten, A., Hoffmann, F., Inagaki, A., Kadasch, E., Kanani-Sühring, F., Ketelsen, K., … Raasch, S. (2020). Overview of the PALM model system 6.0. *Geosci. Model Dev*, *13*, 1335–1372. https://doi.org/10.5194/gmd-13-1335-2020

Martin, T. (2021). *Community Risk, Vulnerability, and Resilience Data Module*.

Marvi, M. T. (2020). A review of flood damage analysis for a building structure and contents. *Natural Hazards*, *102*(3), 967–995. https://doi.org/10.1007/S11069-020-03941-W/TABLES/2

Menk, L., Terzi, S., Zebisch, M., Rome, E., Lückerath, D., Milde, K., & Kienberger, A. S. (2022). Climate Change Impact Chains: A Review of Applications, Challenges, and Opportunities for Climate Risk and Vulnerability Assessments. *Weather, Climate, and Society*, *14*(2), 619–636. https://doi.org/10.1175/WCAS-D-21-0014.1

Mi, L., Shen, L., Han, Y., Cai, C. S., Zhou, P., & Li, K. (2023). Wind field simulation using WRF model in complex terrain: A sensitivity study with orthogonal design. *Energy*, 129411. https://doi.org/10.1016/J.ENERGY.2023.129411

Mohan, P. (2017). The economic impact of hurricanes on bananas: A case study of Dominica using synthetic control methods. *Food Policy*, *68*, 21–30. https://doi.org/10.1016/J.FOODPOL.2016.12.008

Monge, J. J., McDonald, N., & McDonald, G. W. (2022). A review of graphical methods to map the natural hazard-to-wellbeing risk chain in a socio-ecological system. *Science of The Total Environment*, *803*, 149947. https://doi.org/10.1016/J.SCITOTENV.2021.149947

Mortezazadeh, M., Jandaghian, Z., & Wang, L. L. (2021). Integrating CityFFD and WRF for modeling urban microclimate under heatwaves. *Sustainable Cities and Society*, *66*, 102670. https://doi.org/10.1016/J.SCS.2020.102670

Mortezazadeh, M., Wang, L. L., Albettar, M., & Yang, S. (2022). CityFFD – City fast fluid dynamics for urban microclimate simulations on graphics processing units. *Urban Climate*, *41*, 101063. https://doi.org/10.1016/J.UCLIM.2021.101063

Mostafa, K., Zisis, I., & Moustafa, M. A. (2022). Machine Learning Techniques in Structural Wind Engineering: A State-of-the-Art Review. *Applied Sciences 2022, Vol. 12, Page 5232*, *12*(10), 5232. https://doi.org/10.3390/APP12105232

Muñoz-Sabater, J., Dutra, E., Agustí-Panareda, A., Albergel, C., Arduini, G., Balsamo, G., Boussetta, S., Choulga, M., Harrigan, S., Hersbach, H., Martens, B., Miralles, D. G., Piles, M., Rodríguez-Fernández, N. J., Zsoter, E., Buontempo, C., & Thépaut, J.-N. (2021). ERA5-Land: a state-of-the-art global reanalysis dataset for land applications. *Earth Syst. Sci. Data*, *13*, 4349–4383. https://doi.org/10.5194/essd-13-4349-2021

Nasrollahi, N., Aghakouchak, A., Li, J., Gao, X., Hsu, K., & Sorooshian, S. (2012). Assessing the Impacts of Different WRF Precipitation Physics in Hurricane Simulations. *Weather and Forecasting*, *27*(4), 1003–1016. https://doi.org/10.1175/WAF-D-10-05000.1

Nazarian, N., Scott Krayenhoff, E., & Martilli, A. (2019). *A One-Dimensional Model of Turbulent Flow Through "Urban" Canopies: Updates Based on Large-Eddy Simulation*. https://doi.org/10.5194/gmd-2019-230

Nia, K. R., & Mori, G. (2018). Building damage assessment using deep learning and ground-level image data. *Proceedings - 2017 14th Conference on Computer and Robot Vision, CRV 2017*, *2018-January*, 95–102. https://doi.org/10.1109/CRV.2017.54

NOAA. (2023). *Cyclone Hazards & Safety*. https://www.noaa.gov/jetstream/tc-hazards

Nofal, O. M., Amini, K., Padgett, J. E., van de Lindt, J. W., Rosenheim, N., Darestani, Y. M., Enderami, A., Sutley, E. J., Hamideh, S., & Duenas-Osorio, L. (2023). Multi-hazard socio-physical resilience assessment of hurricane-induced hazards on coastal communities. *Resilient Cities and Structures*, *2*(2), 67–81. https://doi.org/10.1016/J.RCNS.2023.07.003

Nofal, O. M., van de Lind, J. W., & Zakzouk, A. (2022). BIM-GIS integration approach for high-fidelity wind hazard modeling at the community-level. *Frontiers in Built Environment*, *8*, 915209. https://doi.org/10.3389/FBUIL.2022.915209/BIBTEX

OAS. (1991). *Primer on natural hazard management in integrated regional development planning | PreventionWeb*. Organization of American States. Dept. of Regional Development and Environment.

https://www.preventionweb.net/publication/primer-natural-hazard-management-integrated-regional-development-planning

Oh, M., Lee, J., Kim, J. Y., & Kim, H. G. (2022). Machine learning-based statistical downscaling of wind resource maps using multi-resolution topographical data. *Wind Energy*, *25*(6), 1121–1141. https://doi.org/10.1002/WE.2718

Pasch, R. J., Penny, A. B., & Berg, R. (2023). HURRICANE MARIA. *NATIONAL HURRICANE CENTER TROPICAL CYCLONE REPORT*.

PDNA. (2017a). *Post-Disaster Needs Assessment Hurricane Maria A Report by the Government of the Commonwealth of Dominica.*

PDNA. (2017b). *Post-Disaster Needs Assessment Hurricane Maria A Report by the Government of the Commonwealth of Dominica.*

Pilkington, S. F., & Mahmoud, H. N. (2017). Real-time application of the multihazard hurricane impact level model for the atlantic basin. *Frontiers in Built Environment*, *3*, 283948. https://doi.org/10.3389/FBUIL.2017.00067/BIBTEX

Pokhrel, R., Cos, S. del, Montoya Rincon, J. P., Glenn, E., & González, J. E. (2021). Observation and modeling of Hurricane Maria for damage assessment. *Weather and Climate Extremes*, *33*, 100331. https://doi.org/10.1016/J.WACE.2021.100331

Roldán, M., Montoya, R. D., Rios, J. D., & Osorio, A. F. (2023). Modified parametric hurricane wind model to improve the asymmetry in the region of maximum winds. *Ocean Engineering*, *280*, 114508. https://doi.org/10.1016/J.OCEANENG.2023.114508

Ruiz-Salcines, P., Salles, P., Robles-Díaz, L., Díaz-Hernández, G., Torres-Freyermuth, A., & Appendini, C. M. (2019). On the Use of Parametric Wind Models for Wind Wave Modeling under Tropical Cyclones. *Water 2019, Vol. 11, Page 2044*, *11*(10), 2044. https://doi.org/10.3390/W11102044

Sanders, R. (2006). *UC Berkeley-led levee investigation team releases final report*. https://newsarchive.berkeley.edu/news/media/releases/2006/05/24_leveereport.shtml

Sapiega, P., Zalewska, T., & Struzik, P. (2023). Application of SWAN model for wave forecasting in the southern Baltic Sea supplemented with measurement and satellite data. *Environmental Modelling & Software*, *163*, 105624. https://doi.org/10.1016/J.ENVSOFT.2023.105624

Sarker, S., & Adnan, M. S. G. (2024). Evaluating multi-hazard risk associated with tropical cyclones using the fuzzy analytic hierarchy process model. *Natural Hazards Research*, *4*(1), 97–109. https://doi.org/10.1016/J.NHRES.2023.11.007

Schaefer, M., Teeuw, R., Day, S., Zekkos, D., Weber, P., Meredith, T., & van Westen, C. J. (2020). Low-cost UAV surveys of hurricane damage in Dominica: automated processing with co-registration of pre-hurricane imagery for change analysis. *Natural Hazards*, *101*(3), 755–784. https://doi.org/10.1007/S11069-020-03893-1/TABLES/2

Silva-Araya, W. F., Santiago-Collazo, F. L., Gonzalez-Lopez, J., & Maldonado-Maldonado, J. (2018). Dynamic Modeling of Surface Runoff and Storm Surge during Hurricane and Tropical Storm Events. *Hydrology 2018, Vol. 5, Page 13*, *5*(1), 13. https://doi.org/10.3390/HYDROLOGY5010013

Singh, J., Kumar Roy, A., Jagbir, S., & Amrit Kumar, R. (2021). *Wind loads on roof of low-rise buildings. 14*(5). https://www.researchgate.net/publication/351282969

Skamarock, W. C., & Klemp, J. B. (2008). A time-split nonhydrostatic atmospheric model for weather research and forecasting applications. *Journal of Computational Physics*, *227*(7), 3465–3485. https://doi.org/10.1016/J.JCP.2007.01.037

Sparks, P. R., Schiff, S. D., & Reinhold, T. A. (1994). Wind damage to envelopes of houses and consequent insurance losses. *Journal of Wind Engineering and Industrial Aerodynamics*, *53*(1–2), 145–155. https://doi.org/10.1016/0167-6105(94)90023-X

Srinivas Kolukula, S., & Murty, P. L. N. (2022). Improving cyclone wind fields using deep convolutional neural networks and their application in extreme events. *Progress in Oceanography*, *202*, 102763. https://doi.org/10.1016/J.POCEAN.2022.102763

Sun, D., Xu, J., Wen, H., & Wang, D. (2021). Assessment of landslide susceptibility mapping based on Bayesian hyperparameter optimization: A comparison between logistic regression and random forest. *Engineering Geology*, *281*, 105972. https://doi.org/10.1016/J.ENGGEO.2020.105972

Syawitri, T. P., Yao, Y. F., Chandra, B., & Yao, J. (2021). Comparison study of URANS and hybrid RANS-LES models on predicting vertical axis wind turbine performance at low, medium and high tip speed ratio ranges. *Renewable Energy*, *168*, 247–269. https://doi.org/10.1016/J.RENENE.2020.12.045

Taghizadeh, S., Witherden, F. D., Girimaji, S. S., Tabib, M., Rasheed, A., & Kvamsdal, T. (2015). LES and RANS simulation of onshore Bessaker wind farm: analysing terrain and wake effects on wind farm performance. *Journal of Physics*. https://doi.org/10.1088/1742-6596/625/1/012032

Tiesi, A., Pucillo, A., Bonaldo, D., Ricchi, A., Carniel, S., & Miglietta, M. M. (2021). Initialization of WRF Model Simulations With Sentinel-1 Wind Speed for Severe Weather Events. *Frontiers in Marine Science*, *8*, 573489. https://doi.org/10.3389/FMARS.2021.573489/BIBTEX

Tilloy, A., Malamud, B. D., Winter, H., & Joly-Laugel, A. (2019). A review of quantification methodologies for multi-hazard interrelationships. *Earth-Science Reviews*, *196*, 102881. https://doi.org/10.1016/J.EARSCIREV.2019.102881

Tossas, L. A. M., & Leonardi, S. (2013). *Wind Turbine Modeling for Computational Fluid Dynamics: December 2010 - December 2012*. https://api.semanticscholar.org/CorpusID:112220433

UNDRR. (2009). *Global assessment report on disaster risk reduction (2009) | UNDRR*. https://www.undrr.org/publication/global-assessment-report-disaster-risk-reduction-2009

UNDRR. (2011). *Global assessment report on disaster risk reduction (2011) | UNDRR*. https://www.undrr.org/publication/global-assessment-report-disaster-risk-reduction-2011

UNDRR. (2013). *Global assessment report on disaster risk reduction 2013 | UNDRR*. https://www.undrr.org/publication/global-assessment-report-disaster-risk-reduction-2013

UNDRR. (2019). *Global assessment report on disaster risk reduction 2019 | UNDRR*. https://www.undrr.org/publication/global-assessment-report-disaster-risk-reduction-2019

UNDRR. (2022). *GAR2022: Our World at Risk (GAR) | UNDRR*. https://www.undrr.org/gar/gar2022-our-world-risk-gar

UNISDR. (2009). *UNISDR Terminology on Disaster Risk Reduction*. www.preventionweb.net

van Westen, C., Kappes, M. S., Luna, B. Q., Frigerio, S., Glade, T., & Malet, J. P. (2014). Medium-scale multi-hazard risk assessment of gravitational processes. *Advances in Natural and Technological Hazards Research*, *34*, 201–231. https://doi.org/10.1007/978-94-007-6769-0_7

Wagner, L. E. (2013). A history of Wind Erosion Prediction Models in the United States Department of Agriculture: The Wind Erosion Prediction System (WEPS). *Aeolian Research*, *10*, 9–24. https://doi.org/10.1016/J.AEOLIA.2012.10.001

Wang, J., He, Z., & Weng, W. (2020). A review of the research into the relations between hazards in multi-hazard risk analysis. *Natural Hazards*, *104*(3), 2003–2026. https://doi.org/10.1007/S11069-020-04259-3/TABLES/2

Wang, J., Wang, L. (Leon), & You, R. (2023). Evaluating a combined WRF and CityFFD method for calculating urban wind distributions. *Building and Environment*, *234*, 110205. https://doi.org/10.1016/J.BUILDENV.2023.110205

Wang, Y., Fang, Z., Hong, H., Costache, R., & Tang, X. (2021). Flood susceptibility mapping by integrating frequency ratio and index of entropy with multilayer perceptron and classification and

regression tree. *Journal of Environmental Management*, *289*, 112449. https://doi.org/10.1016/J.JENVMAN.2021.112449

Wang, Z., Zhao, J., Huang, H., & Wang, X. (2022). A Review on the Application of Machine Learning Methods in Tropical Cyclone Forecasting. *Frontiers in Earth Science*, *10*, 902596. https://doi.org/10.3389/FEART.2022.902596/BIBTEX

Ward, P. J., Blauhut, V., Bloemendaal, N., Daniell, E. J., De Ruiter, C. M., Duncan, J. M., Emberson, R., Jenkins, F. S., Kirschbaum, D., Kunz, M., Mohr, S., Muis, S., Riddell, A. G., Schäfer, A., Stanley, T., Veldkamp, I. E. T., & Hessel, W. C. (2020). Review article: Natural hazard risk assessments at the global scale. *Natural Hazards and Earth System Sciences*, *20*(4), 1069–1096. https://doi.org/10.5194/NHESS-20-1069-2020

Westen, C. van, & Greiving, S. (2017). Multi-hazard risk assessment and decision making. *Books.Google.ComCJ van Westen, S GreivingEnvironmental Hazards Methodologies for Risk Assessment and Management, 2017•books.Google.Com*. https://books.google.com/books?hl=nl&lr=&id=mwZpDgAAQBAJ&oi=fnd&pg=PA31&ots=lYV60jpzou&sig=GZGn1ZNfeYu2jdNaCkDFpSwXw4w

Womble, J. A., Dissertation, B. S. C. E. C. E. A., Mulligan, K., Nutter, B., Liang, D., & Borrelli, A. J. (2005). *Remote-sensing applications to windstorm damage assessment*. Texas Tech University. http://hdl.handle.net/2346/17733

Womble, J. A., Ghosh, S., Adams, B. J., & Friedland, C. J. (2006). *Advanced Damage Detection for Hurricane Katrina: Integrating Remote Sensing Images and VIEWS Field Reconnaissance*. https://api.semanticscholar.org/CorpusID:132112018

Womble, J. A., Smith, D. A., Liang, D., Schroeder, J. L., Brown, T. M., & Mehta, K. C. (2010). Imagery-based wind damage functions. *Structures Congress 2010*, 1099–1108. https://doi.org/10.1061/41130(369)100

World Meteorological Organization. (2022). *Tropical Cyclones*. https://public.wmo.int/en/our-mandate/focus-areas/natural-hazards-and-disaster-risk-reduction/tropical-cyclones

Wu, T., & Snaiki, R. (2022). Applications of Machine Learning to Wind Engineering. *Frontiers in Built Environment*, *8*, 811460. https://doi.org/10.3389/FBUIL.2022.811460/BIBTEX

Wu, Y.-H. (Eva), Hung, M.-C., Wu, Y.-H. (Eva), & Hung, M.-C. (2016). Comparison of Spatial Interpolation Techniques Using Visualization and Quantitative Assessment. *Applications of Spatial Statistics*. https://doi.org/10.5772/65996

Yu, E., Bai, R., Chen, X., & Shao, L. (2022). Impact of physical parameterizations on wind simulation with WRF V3.9.1.1 under stable conditions at planetary boundary layer gray-zone resolution: a case study over the coastal regions of North China. *Geoscientific Model Development*, *15*(21), 8111–8134. https://doi.org/10.5194/GMD-15-8111-2022

Zeng, H., Talkkari, A., Peltola, H., & Kellomäki, S. (2007). A GIS-based decision support system for risk assessment of wind damage in forest management. *Environmental Modelling & Software*, *22*(9), 1240–1249. https://doi.org/10.1016/J.ENVSOFT.2006.07.002

Zhang, W., Zhao, H., Chen, G., & Yang, J. (2023). Assessing the performance of SWAN model for wave simulations in the Bay of Bengal. *Ocean Engineering*, *285*, 115295. https://doi.org/10.1016/J.OCEANENG.2023.115295

10. DATA MANAGEMENT PLAN

Dataset	NAME OF DATA FILE	SOURCE (PRIMARY OR SECONDARY DATA)	IF SECONDARY, WHO IS THE OWNER?	RESTRICTIONS AND LICENSE	DATA FORM	DATA FORMAT	YEAR OF DATA	CONTAINS PERSONAL DATA (Y/N)	Links
DEM	DEM/Copernicus	Secondary	Copernicus	Open data policy	Raster	.tiff	2017	No	Collections - Copernicus
	DEM/LiDAR		UNDP						
Wind parameters	ECMWF/ERA5	Secondary	ECMWF	Open data policy	Raster	.tiff	2017	No	Datasets | ECMWF
	NOAA/HURDAT2		NOAA						HURDAT2
Building footprint	WSF/EOC	Secondary	German Aerospace Centre	Open data policy	Vector	.shp	2017	No	World Settlement Footprint (WSF)
Land-use	Dominica/CarLand	Secondary	Caribbean Land cover project	Closed data policy	Raster	.tiff	2018	No	
	Dom/WorldCover		ESA	Open data policy	Vector	.shp			https://esa-worldcover.org/en
Landslide map	Dom/landslide	Secondary	ITC (Published by UNDP)	Closed data policy	Vector	.shp	2017	No	
Flood hazard	Dom/flood				Raster	.tiff	2017	No	
Building characteristics	Dom/BDA	Secondary	UNDP	Closed data policy	Vector	.shp	2017	Yes	

11. APPENDIX A: COLUMNS FOR BUILDING INFORMATION

Red highlighted columns are used for choice of households to visit during field survey as mentioned in section 5.2

ResponseId	PrimaryOccupantAge	RoofDamage	Walls_Other_text
TagLabel	Secondary Occupant	RoofMaterials_Age	Floor_Damage
Color Tag	SecondaryOccupantFamilyName	RoofMaterials_Cement	Floor_Concrete
Assessment Date	SecondaryOccupantName	RoofMaterials_GalvanizeSheeting	Floor_Timber
Parish	SecondaryOccupantGender	RoofMaterials_Other	Floor_other_text
Community	SecondaryOccupantAge	RoofMaterials_OtherSpecifed	Ceiling_Damage
Latitude	Count of Adults	RoofMaterials_Pvf2Sheeting	Ceiling_type_Exposed
Longitude	Count of Women	RoofMaterials_ReinforcedConcrete	Ceiling_type_Suspended
BuildingOccupation	Count of Men	RoofMaterials_Shingle	Ceiling_type_Other_text
Public_Private	Count of Children	RoofType_Flat	Ceiling_Finish_Damage
StructureUse	Count of Girls	RoofType_CrossHipped	Ceiling_Finish_Concrete
PrivateStructureType	Count of Boys	RoofType_Gable	Ceiling_Finish_Plywood
PublicStructureType	Count of Elderly	RoofType_Hip	Ceiling_Finish_Sheetrock
PublicStructureType_other_text	Count of Disabled	RoofType_HipAndValley	Ceiling_Finish_Other_text
Insurance	BuildingSize	RoofType_LeanTo	Hazards
RepairsDone	Height	RoofType_Other	Hazards_other
LandTitle	Width	RoofType_OtherSpecified	Materials_Bricks
LandTitle_other	Length	RoofType_Pyramid	Materials_Concrete
OccupantsAvailable	Nb_floors	RoofType_Shed	Materials_Timber
Owner_availability	Main_Damage_Type_Roof	Walls_Damage	Materials_IronBars
Primary Occupant	Main_Damage_Type_Walls	Walls_Plywood	Materials_Stone
PrimaryOccupantFamilyName	Main_Damage_Type_Structure	Walls_rendered_Walls	Materials_Tin
PrimaryOccupantName	Main_Damage_Type_Service	Walls_Timber_Boards	
PrimaryOccupantGender	Main_Damage_Type_Other_text	Walls_Timber_concrete	

12. APPENDIX B: QUESTIONNAIRE

Hello, I am a student from University of Twente, the Netherland doing my master's research on the different hazard interaction during tropical cyclone Maria, 2017. All the answers you give are confidential and are solely for research purposes. Your names and locations will not be revealed in my research.

Date: Region: Location:

Observations and Perceptions:

1. What did you observe first: flood, landslide or very high wind speeds during the cyclone?
2. Do you remember the direction from which the flood/landslide came?
3. Do you remember the direction from where the wind started blowing?
4. Was the wind very gusty and strong throughout the cyclone period? If not can you please describe how and when it changed after hurricane started?
5. When did precipitation start, before or after wind blowing started?
6. How high was the flood height respective to your house? How long did the water remain that high?
7. Did you experience any wind damage on your house, e.g. roof damaged, or walls damaged? If yes, what were the areas of your house that were affected due to flood?
8. Did wind blow off your house roof? If so, was it before or after flood/landslide occurred and how big was that time gap? Can you describe me the incident when this happened.
9. Can you recall the time gap between starting of rainfall and flood occurrence? Can you describe me the incident when you saw flood arriving after rainfall.
10. Was there landslide at your place? If yes, how long did it take landslide to occur at your place after the staring of rainfall? Can you describe the landslide that happened and how did it affect evacuation and local infrastructures.
11. What impact did the wind have on local buildings and structures?
12. What impact did the flood have on local buildings and structures?
13. What impact did the landslide have on local buildings and structures?
14. Were there any construction going on, in and around the neighborhood? If yes, where was that rubble or pile of construction material situated?
15. Did the construction have any impact on the blocking of roads? Was the blocking material just construction material or building rubble, trees and mud accumulated later on?
16. Was any rubble from previous construction lead to blocking of drainage? Did it cause more flood?
17. Were there instances where one hazard (e.g., flooding) worsened another (e.g., landslides)?
18. Was the electricity cut-off by the government? If not, do you remember any power outage or short-circuit in your area?
19. Do you think the combination of high wind speeds and precipitation made the damage worse? If yes, why?

Communication and Warning Systems:

20. How effective were the communication and warning systems in place during the cyclone?
21. How do you seek shelter during cyclones? Is it provided by government or are there pre-determined rules for evacuation?

Post-Cyclone Recovery:

22. What was the major challenge you focused post-cyclone? What impact did you reduce the most? Wind/flood/landslide debris?

APPENDIX

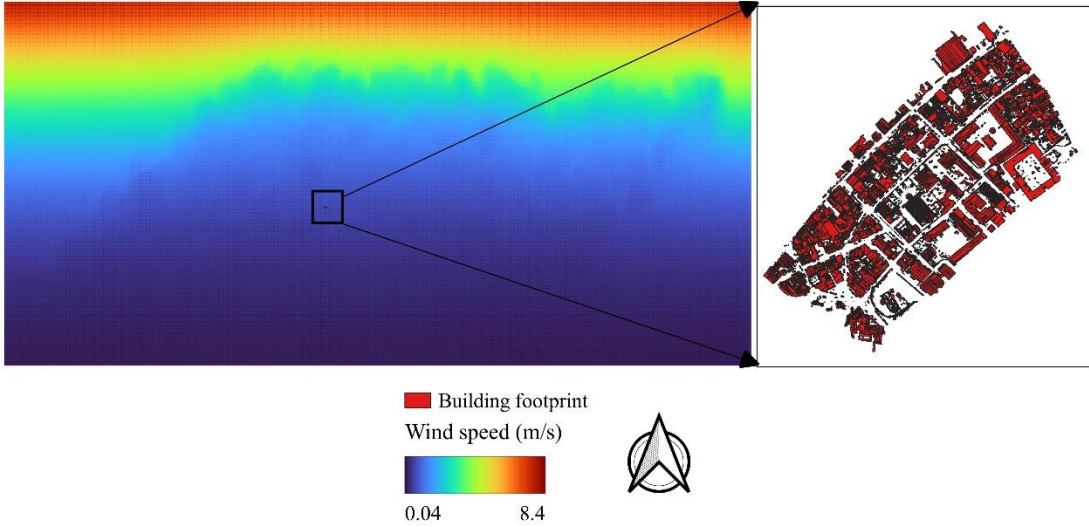Government officials questions: **Not to citizens**

23. What were the major regions that were affected during the cyclone?
24. Which hazard: flood/landslide/wind caused more damage?
25. Which regions were more affected due to uprooting of trees?
26. Which regions were more affected due to landslide?
27. Which regions were more affected due to flood and water logging?
28. Were there any major construction going on which led to blockage of roads/ evacuation routes?
29. How would you say TC Maria was different from the previous cyclones happening in the past?
30. Based on your experience, what long-term strategies do you think could enhance the community's resilience to multi-hazard events in the future?

13. APPENDIX C: FIELD ITINERARY

Date	Day	Activities
12-Feb	Monday	Interview at Portsmouth
13-Feb	Tuesday	Interview at Grande Bay & Nearby
14-Feb	Wednesday	Meeting at Red Cross Division Roseau Meeting at CREAD
15-Feb	Thursday	Meeting w/ Office of Disaster Management
16-Feb	Friday	Interview at Scotts Head, Point Michel
17-Feb	Saturday	Interview at Grande Bay & Pichelin
18-Feb	Sunday	Extra citizens' interview in Roseau

14. APPENDIX D: OVERLAY MAP

15. APPENDIX E: LOCATION